

Article

Design Criteria and Accommodating Capacity Analysis of Vertiports for Urban Air Mobility and Its Application at Gimpo Airport in Korea

Byeongseon Ahn and Ho-Yon Hwang * 

Department of Aerospace Engineering, and Convergence Engineering for Intelligence Drone, Sejong University, 209, Neungdong-ro, Gwangjin-gu, Seoul 05006, Korea; qudtjs1540@sju.ac.kr

* Correspondence: hyhwang@sejong.edu; Tel.: +82-10-6575-2282

Abstract: This study establishes design criteria for touchdown and liftoff (TLOF) pads, final approach and takeoff (FATO), safety areas, gates, and taxiways, which are components necessary for the operation of vertiports for urban air mobility (UAM), and analyzed vertiport capacity compliant with the arrangement of the components in a limited space. We used new vertiport design regulations from the Federal Aviation Administration (FAA) and European Union Aviation Safety Agency (EASA) for the vertiport design criteria. Vertiport components were sized based on Hyundai Motor's S-A1 aircraft, and the layouts were classified as linear, satellite, and pier according to the arrangement of the TLOF pad and gate. The characteristics of each layout were analyzed for the same area. Based on these layouts, the parking space of Gimpo Airport that will be used for operating airport shuttles in the Seoul metropolitan area was measured and each layout was arranged to validate the characteristics of the layouts. Using the MATLAB program, we selected the most efficient layout among linear, satellite, and pier layouts, and estimated the TLOF pad and gate utilization rate. In addition, we evaluated the capacity of the two-story vertiport proposed by the Korea Airports Corporation for efficient use of space.

Keywords: UAM; vertiport; eVTOL; TLOF pad; FATO; vertiport layout; vertiport capacity



Citation: Ahn, B.; Hwang, H.-Y. Design Criteria and Accommodating Capacity Analysis of Vertiports for Urban Air Mobility and Its Application at Gimpo Airport in Korea. *Appl. Sci.* **2022**, *12*, 6077. <https://doi.org/10.3390/app12126077>

Academic Editor: Wei Huang

Received: 6 March 2022

Accepted: 11 June 2022

Published: 15 June 2022

Publisher's Note: MDPI stays neutral with regard to jurisdictional claims in published maps and institutional affiliations.



Copyright: © 2022 by the authors. Licensee MDPI, Basel, Switzerland. This article is an open access article distributed under the terms and conditions of the Creative Commons Attribution (CC BY) license (<https://creativecommons.org/licenses/by/4.0/>).

1. Introduction

Currently, many companies such as airplane manufacturers, automobile manufacturers, and information technology companies are developing urban air mobility (UAM) as a way to solve the problem of saturation of ground transportation in major cities in the world. By operating battery-powered electric vertical takeoff and landing (eVTOL) vehicles in the urban area, UAM is expected to be widely used in the near future for not only reducing commuting time but also solving environmental problems such as emissions and noise. Therefore, along with the development of eVTOL aircraft, it is necessary to study the design criteria of vertiports to accommodate and operate eVTOL aircraft and to evaluate passenger-carrying capacities.

The National Aeronautics and Space Administration (NASA) analyzed the characteristics of locations for operating VTOL aircraft along with available spaces such as floating barges and highway interchanges, considering private land, wind, takeoff distance, and noise for the Silicon Valley region [1]. At the 2018 Uber Elevate Summit, various designs of vertiport shapes were presented by several companies, including architecture firms such as Gannett Fleming and Humphreys & Partners Architects [2–5]. In addition, in 2019, BOKA Powell selected two locations, downtown Dallas and Frisco in Texas, and presented “Uber Air 2023 Skyport Mobility Hub Concepts” and offered a specific design that accommodates electric vehicles and electric scooter charging stations [6].

Parker D. Vascik et al. [7] reviewed the existing heliports to determine the size and arrangement of the vertiport components and modeled the vertiport using the infrastruc-

ture variables (TLOF pads, gates, and staging stands) and operating parameters (time for taxiing, turnaround, arrival and departure, pre-staged aircrafts, and operating policy). Gurobi 8.0.1 solver and Python 3.6.6 were used to analyze the formulated model using integer programming. Different from the reference [7] method, which calculates all possible cases for a specific time, in that study, a method that determines the acceptable maximum range by plotting an outer line only was implemented using the MATLAB [8]. Shannon Zelinski et al. [9] defined spacing constraints as prescribed for general aviation visual flight rules (VFR) heliports in [10] and defined perimeter design, central design, and disconnected design for different square spaces and then compared utilization rates. Nelson M. Guerreiro et al. [11] analyzed the UAM demand scenario where external entities (passengers) use a vertiport reservation system in the near future. Scenarios were classified as a simulation model and a queuing model, and the vertiport for various environments was compared and analyzed by applying the first-come and first-served (FCFS) scheduling algorithms. M. H. Vázquez et al. [12] presented a method based on integer programming, which created a vertiport design automatically for a given area. In that study, more than 25 million combinations of the different parameters were obtained and analyzed. F. Knabe et al. [13] defined an exemplary vertidrome concept, namely, a linear independent expandable drive-through (LIEDT) topology, as well as operating and traffic rules for arriving and departing vehicles.

In this study, the Hyundai S-A1 eVTOL aircraft was applied to the vertiport design regulations to study the location-based vertiport capacity analysis and design criteria. Moreover, since UAM mainly pertain to urban areas where a vertiport may be installed in a limited space, vertiport components were laid out according to the actual space, and the capacity of each layout was compared using the MATLAB program. Finally, we chose the most efficient arrangement for the space and calculated the number of passengers per hour.

2. Components of Vertiport

2.1. Vertiport Component Sizing

Among UAM infrastructure operating in urban areas, a vertiport has a limited number of components because it cannot be allocated a large space like an existing airport or heliport. Vertiport components are composed of TLOF pads, gates, induction paths, and so forth. We investigated various arrangements of components by referencing studies from the literature from the FAA and EASA. The FAA announced that they are discussing with EASA and ICAO about the vertiport installation standards, such as the TLOF, FATO, and safety area based on the maximum aircraft dimensions. The controlling dimension (CD) is the longest distance between the two outermost opposite points on the aircraft (e.g., wingtip-to-wingtip, rotor tip-to-rotor tip, rotor tip-to-wingtip, or fuselage-to-rotor tip), measured on a level horizontal plane that includes all adjustable components extended to their maximum outboard deflection [14]. EASA [15] classifies VTOL-capable aircraft as an enhanced category, and the standards for these are described in SC-VTOL-01. EASA uses the term 'D-value' to define the limiting dimension. 'D' represents the diameter of the smallest circle that surrounds the VTOL aircraft projection and contains the radius of the rotation of the rotor on the horizontal plane when the aircraft is in takeoff and landing configuration. Basically, both the FAA and EASA classify VTOL aircraft as small helicopters with an MTOW of less than 3175 kg (7000 pounds), but regulations of the two agencies for the vertiport are described differently. Thus, in each section, we applied both regulations separately.

In this study, to provide a sufficient margin (e.g., considering rotor pitch), the size of the vertiport components was determined based on the size of the Hyundai S-A1 diagonal length, which is classified as a large eVTOL aircraft. The rectangular projected area of the S-A1 is 15 m × 10.7 m, so the 18.4 m diagonal length of the rectangle is designated as the CD.

When determining the size of the vertiport TLOF pad, as shown in Figure 1, we used a circular TLOF pad made by the CD because a circular shaped pad could be more recognized by a pilot than a square or rectangular shape in an urban environment [10].

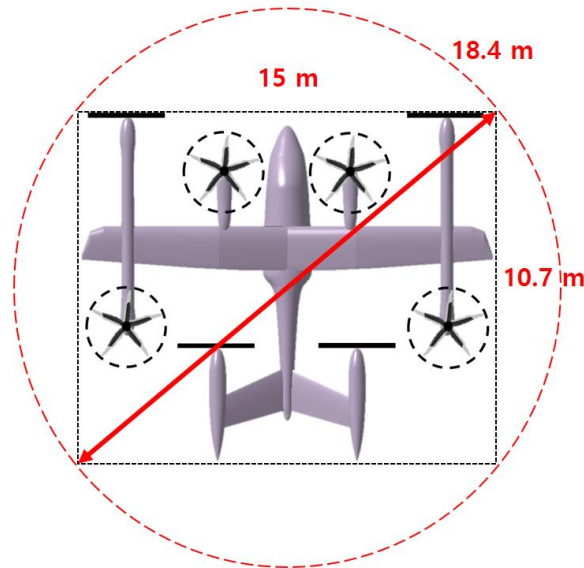


Figure 1. Size of TLOF pad for S-A1.

The TLOF pad is a load-bearing, generally paved area, on which the VTOL aircraft takes off and lands. According to the engineering brief (EB), the landing area design and geometry includes the TLOF, the FATO, and the safety area [14], as shown in Figure 2. In the FATO area, it should be clear with no penetrations or obstructions except for navigational aids that are fixed-by-function, which must be on frangible mounts. To prevent a short circuit or lighting strike, a concrete surface is recommended on elevated TLOFs. In the case of elevated heliports with reinforced concrete construction of TLOF/FATO, cases of autopilot and avionics failure have been reported in some types of helicopters due to the creation of a strong magnetic field in the reinforced concrete slab. This could be an issue for UAM with advanced avionics. The imaginary surfaces for heliports are applicable to vertiports and include the primary surface, approach, and transitional surfaces. In a vertiport, the primary surface is the FATO.

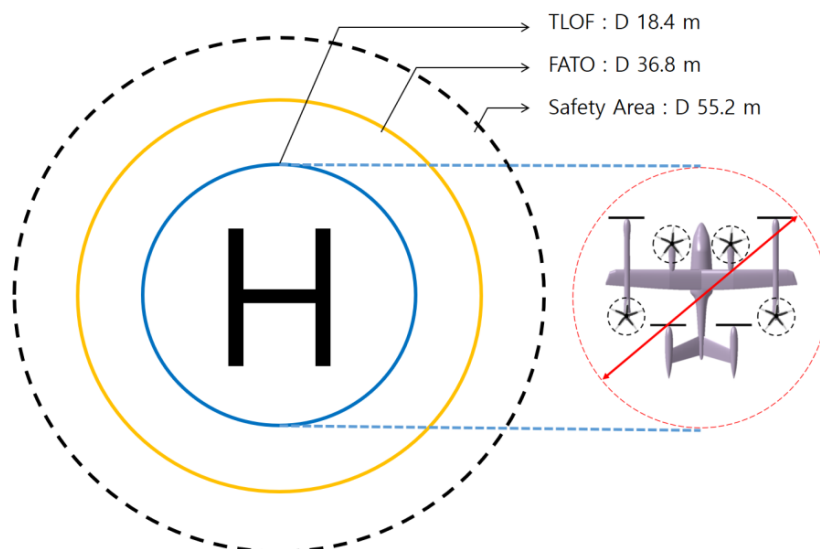


Figure 2. Vertipad size for S-A1 that comply with the FAA’s new regulations.

A vertiport needs to be provided with at least one FATO. The minimum width of a FATO is at least two times the CD of the design helicopter but not less than 100 ft (30.5 m) VTOL aircraft [14]. At elevations above 1000 ft mean sea level (MSL), a longer FATO is required to provide an increased safety margin and greater operational flexibility [10]. The safety area extends outward on all sides of the FATO for a distance of at least one-half the CD and is not necessarily a solid [14]. The size of the TLOF pad is 18.4 m, the FATO is 36.8 m, and the safety area is 55.2 m as shown in Figure 2. The EASA [15] regulates the minimum dimensions of the TLOF as 0.83 CD, the FATO as 1.5 CD, and the safety area as the area extended by the greater distance of 3 m or 0.25 CD to the FATO. If the size of the vertiport component is determined according to the EASA regulations, the TLOF pad, the FATO, and the safety area are 15.272 m, 27.6 m, and 33.2 m, respectively, as shown in Figure 3.

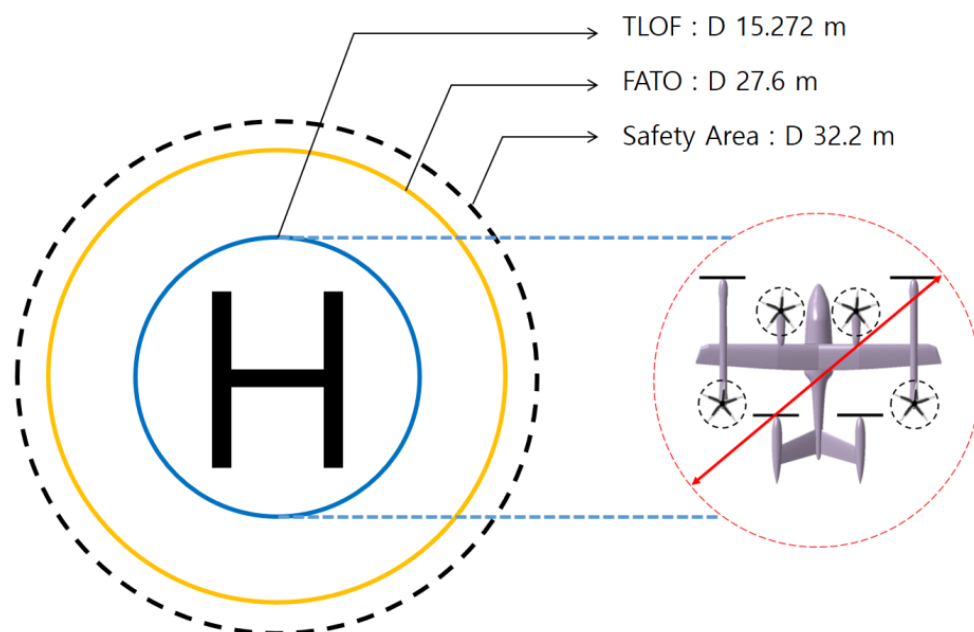


Figure 3. Vertipad size for S-A1 that comply with the EASA's new regulations.

A vertiport supports aircraft takeoff and landing on a vertipad, parking at the gate, passengers getting on and off, recharging, and it can additionally support MRO (maintenance, repair, and overhaul) or aircraft lifting depending on the situation.

Since the FAA has not yet formulated rules for vertiport gates, we made assumptions about gate size based on existing heliport rules. The size of the gate depends on the number and size of the specific aircraft to be accommodated. It is not necessary that every gate accommodate the design helicopter. However, the design helicopter is used to determine the separation between gates and taxiways, and the minimum clearance length is one-third CD. Regardless of helicopter size, the minimum clearance between the tail rotor arcs is 10 ft for ground taxi operations. Ground taxi turns of wheeled helicopters are significantly larger than a hover turn [10]. Therefore, the vertiport in this study does not have a separate apron, and additionally supports recharging, passenger embarking/disembarking, and turnaround and has a 21.4 m maximum gate size by adding 10 ft to the CD as shown in Figure 4.

The EASA [15] also regulates the area supporting the loading or unloading of passengers and cargo, and parking, recharging, and maintenance as 'stand'. The stand should provide a circular area with a size of 1.2 times the maximum aircraft dimensions as shown in Figure 5. The EASA also regulates geometry-based stands that include a 3 m protection area.

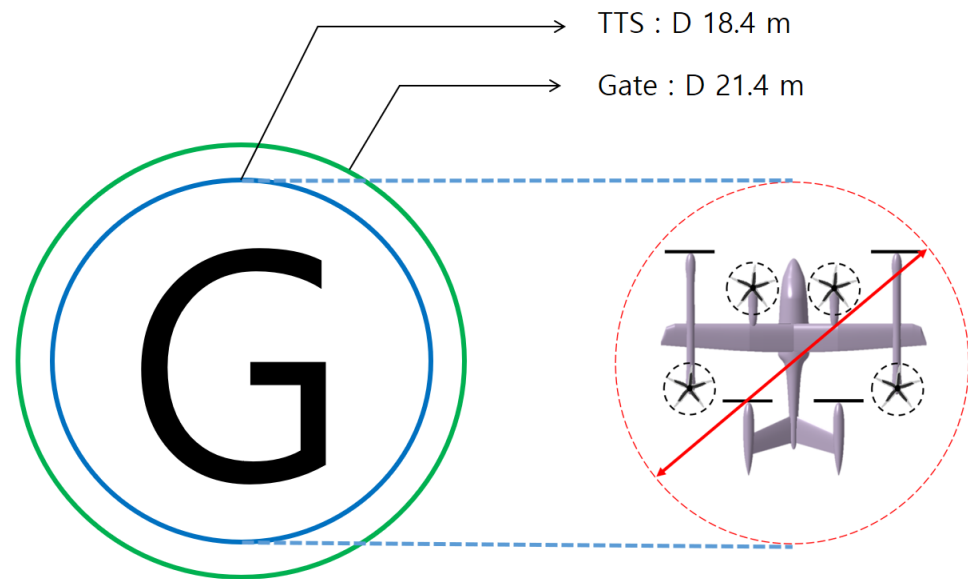


Figure 4. Gate size for S-A1 that comply with the FAA’s new regulations.

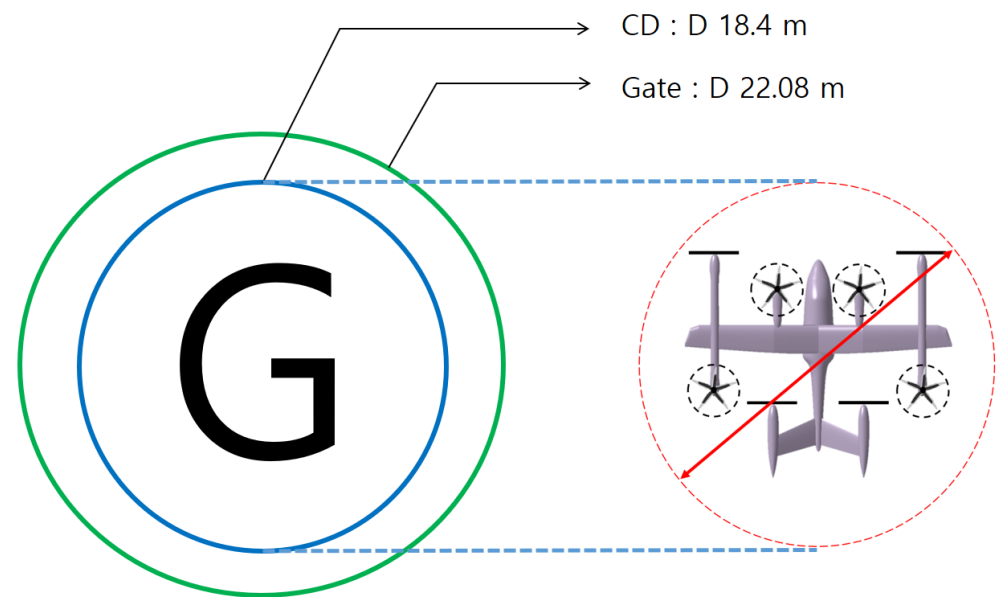


Figure 5. Gate size for S-A1 that comply with the EASA’s new regulations.

According to a study on ramp operation of commuter VTOL aircraft [16], passengers are not allowed to embark and disembark at the runway when the aircraft’s propellers are operating within 200 ft, but the condition was not considered by assuming that eVTOL aircraft does not operate propellers while the passengers are embarking and disembarking.

The FAA’s EB noted that taxiing is an acceptable practice in vertiports and that the EB revision will provide guidance for vertiport taxiways, taxiways, and helicopter parking. According to AC 150/5390-2C [10], the dimensions of taxiways are a function of helicopter size and type of taxi operations. For the ground taxiways covered in this study, cement, concrete, asphalt, or stabilized surfaces, such as turf, must be provided in accordance with the standards of items P-217 of AC 150/5370-10 [17]. This standard meets the pavement guidelines applicable to the TLOF and FATO in a new document from the FAA. Because taxiways are very close to the touchdown and liftoff areas, for unpaved portions, a turf cover must be provided or the surface must be treated in some way to prevent dirt and debris from being raised by a taxiing VTOL aircraft’s rotor wash. Clearance must be secured on both sides of the taxiway so that the minimum size is twice the size of the design aircraft

or 1.5 times the rotor diameter. Since hover guidance requires twice the rotor diameter and ground guidance requires 1.5 times the rotor diameter [10], the overall width of the taxiway was determined to be 27.6 m, which is 1.5 times the CD as shown in Figure 6. According to EASA regulation, the transverse slope of a VTOL-capable aircraft taxiway should not exceed 2 percent and the longitudinal slope should not exceed 3 percent. The ground taxi-route should have a minimum width of 1.5 times the overall width of the largest VTOL aircraft [15], so that the width of the taxiway is also 27.6 m.

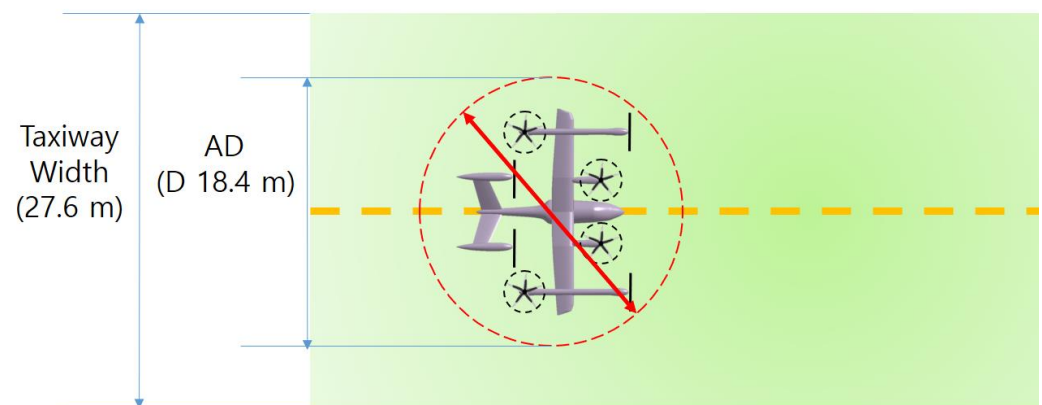


Figure 6. Taxiway width for S-A1.

Tables 1 and 2 summarize the regulations and sizes of the components used in the vertiport capacity analysis.

Table 1. Regulation and dimensions of primary vertiport components that comply with the FAA’s new regulations.

| Components | Regulation | Dimension |
|---------------|--|-----------|
| TLOF pad | CD | 18.4 m |
| FATO | $2 \times CD$ | 36.8 m |
| Safety Area | $3 \times CD$ (1/2 CD added to edge of FATO) | 55.2 m |
| Gate | CD + 10 ft | 21.4 m |
| Taxiway Width | CD + 1/2 CD | 27.6 m |

Table 2. Regulation and dimensions of primary vertiport components that comply with new EASA regulations.

| Components | Regulation | Dimension |
|---------------|------------------------------------|-----------|
| TLOF pad | $0.83 \times CD$ | 15.272 m |
| FATO | $1.5 \times CD$ | 27.6 m |
| Safety Area | FATO + max(3 m, $0.25 \times CD$) | 32.2 m |
| Gate | $1.2 \times CD$ | 22.08 m |
| Taxiway Width | $1.5 \times CD$ | 27.6 m |

2.2. Other Constraints for Vertiport Components

According to the FAA [14], an approach/departure surface is centered on each approach/departure path, and the approach/departure path starts at the edge of the FATO and slopes upward at 8:1 for a distance of 4000 ft (1219 m) where the width is 500 ft (152 m) at a height of 500 ft (152 m) above the vertiport elevation. The transitional surfaces extend outward and upward from the lateral boundaries of the primary surface and from the approach surfaces at a slope of 2:1, horizontal units and vertical units, respectively, for 250 ft (76 m) measured horizontally from the centerline of the primary and approach surfaces [14].

When one TLOF supports takeoff and landing in multi-directions, at least 135 degrees is required between two surfaces. The area below the approach/departure surface should

be clear of penetrations and obstructions to the approach/departure and transitional surfaces [14]. This is an important standard that should be applied to existing objects and newly installed structures in urban areas. The application of the rules for access routes and transition surfaces and airspace is explained with the figures in Section 3.

A 60 m separation distance between two FATOs has been recognized as a reference for simultaneous helicopter landings and takeoffs where the courses to be flown do not conflict and where the MTOW of the helicopter does not exceed 3175 kg. This distance can be used as a reference for conducting a safety assessment to determine whether the distance for VTOL capable aircraft should be adapted [15].

The approach/departure surface and the transitional surface with a 1:8 slope are shown in Figure 7. The dimensions of an omnidirectional obstacle-free volume is shown in Figure 8.

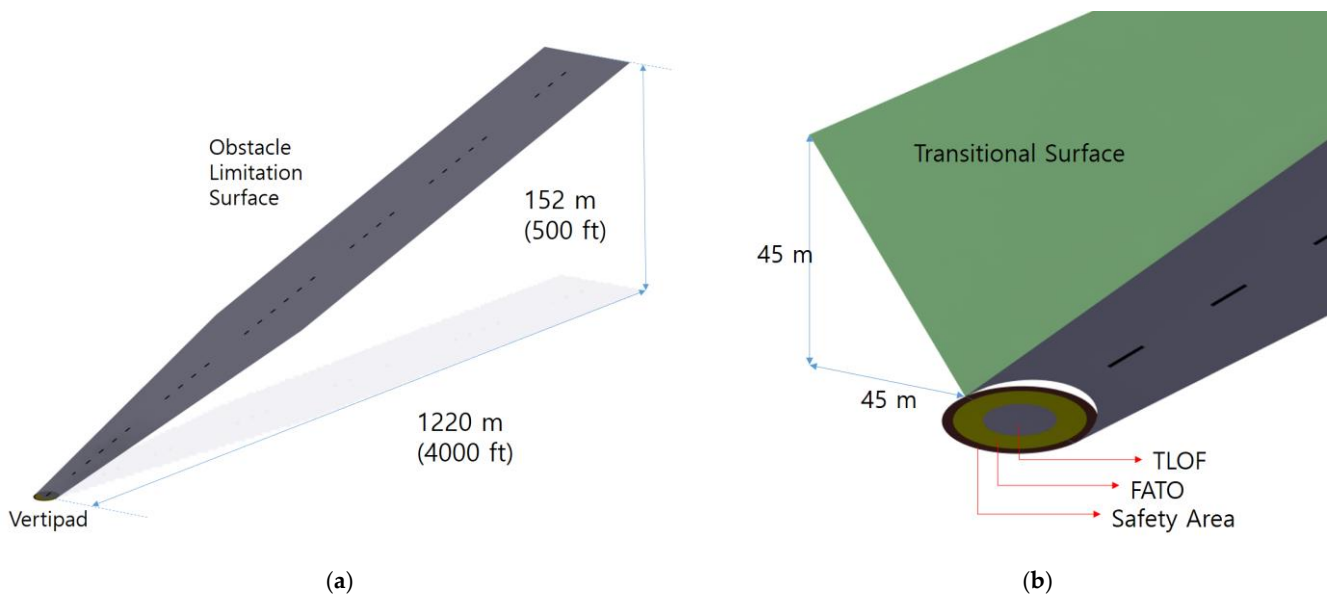


Figure 7. Approach/departure surface and transitional surface with a 1:8 slope: (a) approach/departure surface; (b) transitional surface.

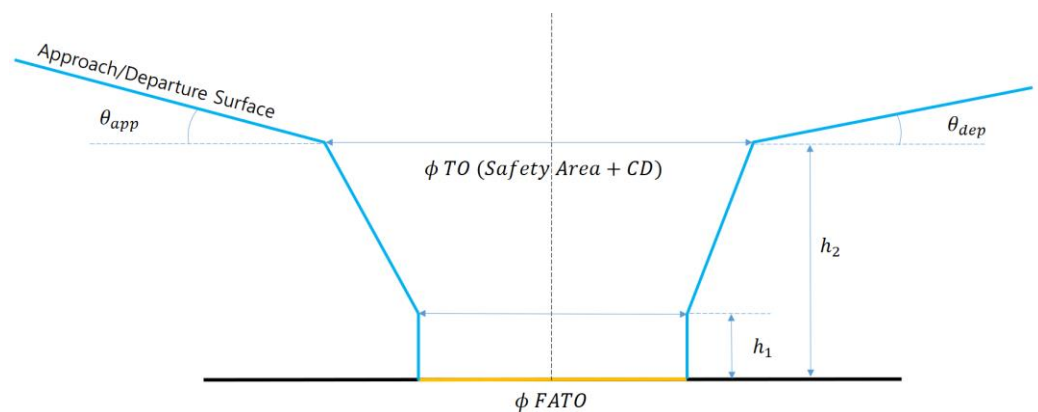


Figure 8. Dimensions of an omnidirectional obstacle-free volume.

According to FAA Joint Order 7110.65Z, Section 3-11-5 [18], aircraft can perform simultaneous takeoffs or landings from TLOF pads with more than a 200 ft centerline separation, and the U.S. Army carries out an operation from TLOF pads 150 ft apart [7]. If there is more than one FATO in a heliport, AC 150/5390-2C [10] recommends that multiple aircraft be operated simultaneously by designating the minimum distance between the FATO perimeters as 200 ft (61 m) to separate the perimeters of the two FATOs so that the safety areas do not overlap.

In this study, the minimum distance between the FATO perimeters was set to 61 m (200 ft) and the minimum distance between the perimeters of the safety area was set to 42.6 m.

2.3. Comparison of Topologies

This section compares the linear, satellite, and pier layouts that we applied for the same area to comply with the FAA's and EASA's new regulations. First, the minimum area required for each layout of the vertiport was determined using the sizes of the TLOF pad and gate. For satellite topology and pier topology, the area was designed to be capable of holding at least two gates per one TLOF pad. According to the FAA's and EASA's new regulations, the standard area required in common for the three deployments is 15,850.56 m² and 7384.8 m², respectively, and the linear, satellite, and pier layout configurations were determined by applying the previously defined vertiport component sizes. When the linear topology tends to support takeoff and landing in one direction, the transition surface is as shown in Figures 9 and 10. For satellite and pier topologies that support relatively multidirectional takeoff and landing, the preferred approach/departure surface is based on the predominant wind direction. Where a reciprocal approach/departure surface is not possible in the opposite direction, it is recommended to use a minimum 135-degree angle between the two surfaces [14].

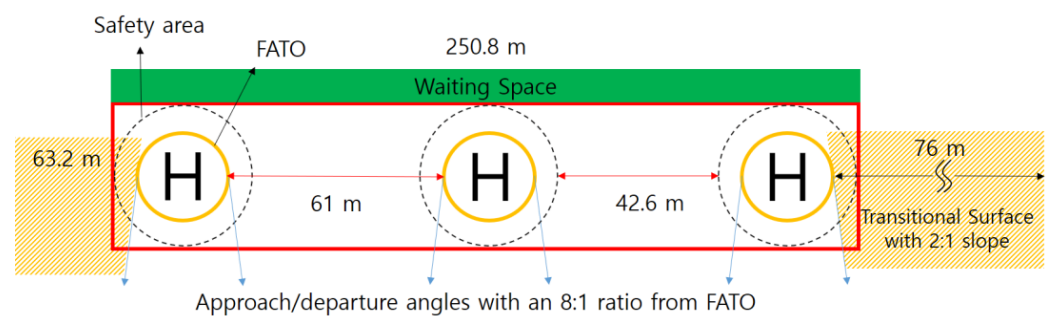


Figure 9. Example of linear topology that complies with the FAA's new regulations.

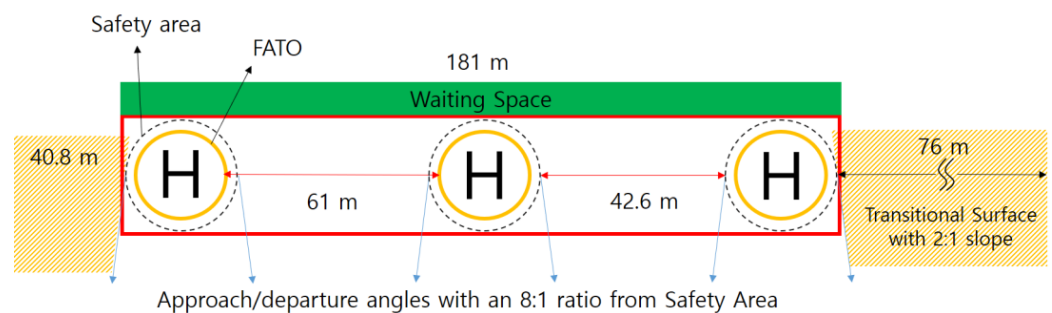


Figure 10. Example of linear topology that complies with the EASA's new regulations.

In a linear topology, several TLOF pads are usually arranged in a row, which is efficient for thin and long spaces such as along a seaside or a riverside. This topology has an advantage when TLOF pads are without gates. Each TLOF pad can take the role of a gate and this arrangement is relatively simple. However, it is necessary to secure additional space in the other than takeoff and landing directions when this topology is installed on a single or lower floor. Therefore, it is necessary to secure additional space in accordance with the approach/departure surface and path regulations in reference [9], considering the height of the structures that may interfere with takeoff and landing around the TLOF pad. An example of a linear topology with a TLOF pad is shown in Figures 9 and 10.

The satellite topology is suitable for a square or circle space, such as SHoP's Architects' Arc' skyport [19], in which one or more TLOF pads are surrounded by several gates. As shown in Figures 11 and 12, the gate is highly utilized because the length of the taxiways is

constant. However, this method has constraints in taking off and landing in the direction of the gate and in integrating with the existing infrastructure.

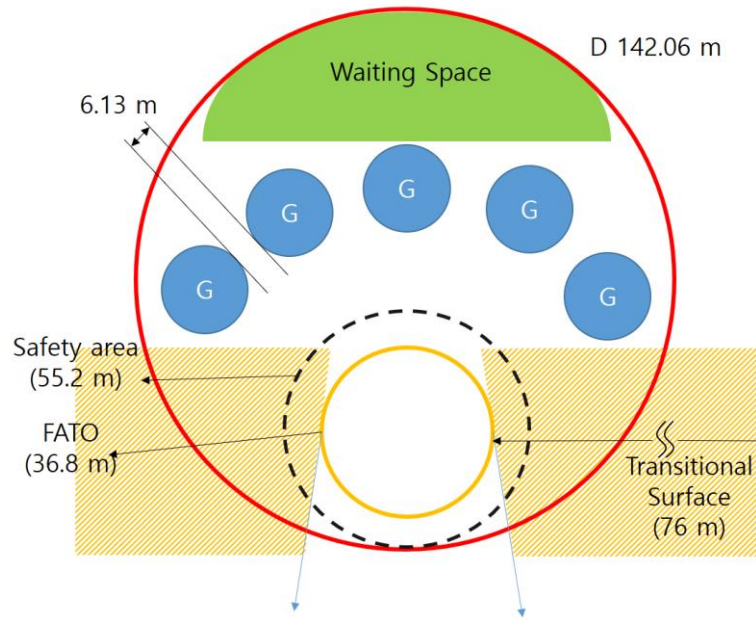


Figure 11. Example of satellite topology that complies with the FAA’s new regulations.

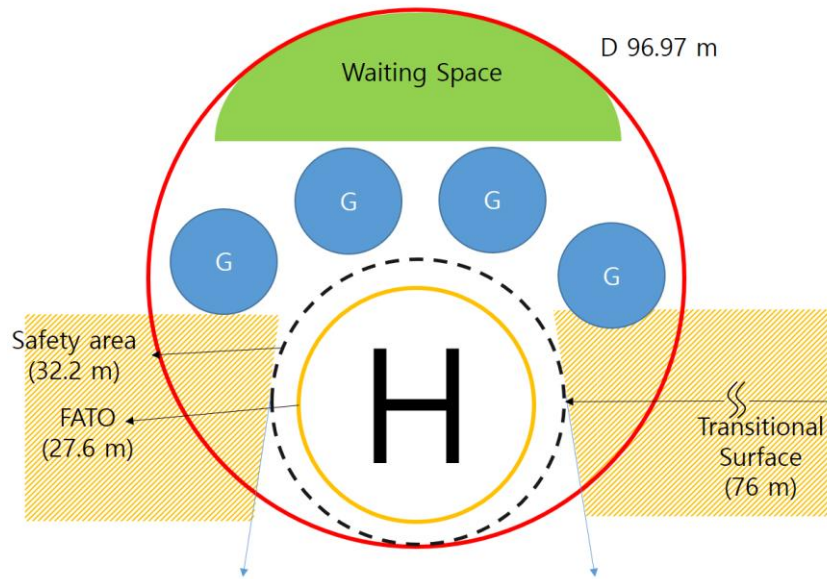


Figure 12. Example of satellite topology that complies with the EASA’s new regulation.

The pier topology has an intermediate rectangular form between a linear topology and a satellite topology. This layout separates the area of the TLOF and the gate to make the takeoff and landing angles at the TLOF pad wider, and a large number of gates can increase the gate utilization. However, since this arrangement shares one taxiway, aircraft turnaround times may be extended and the gate area may be congested. To overcome these problems, a high-level flight air traffic control (ATC) system or two or more taxiways is necessary. A minimum space example of the pier layout providing a multidirectional approach/departure path is shown in Figures 13 and 14. The minimum space was not mentioned in the EASA’s new regulation [15], except for the protection area, which is 1.2 times CD.

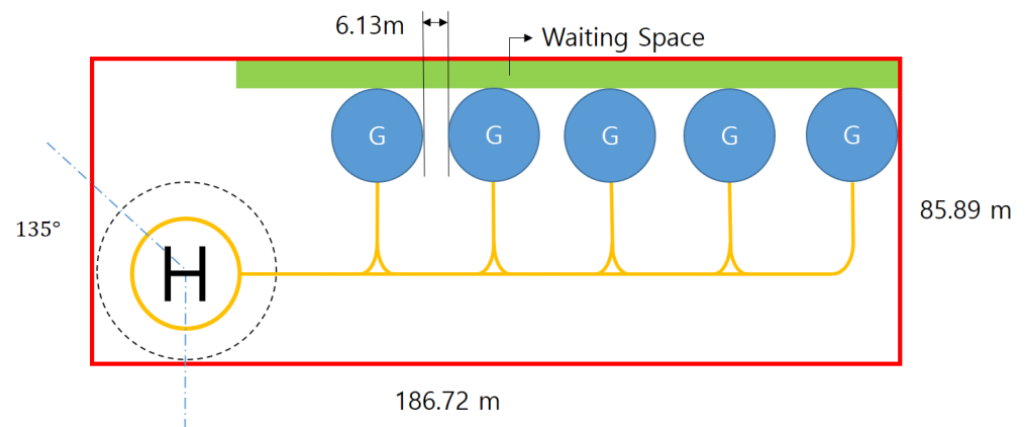


Figure 13. Example of pier topology that complies with the FAA's new regulations.

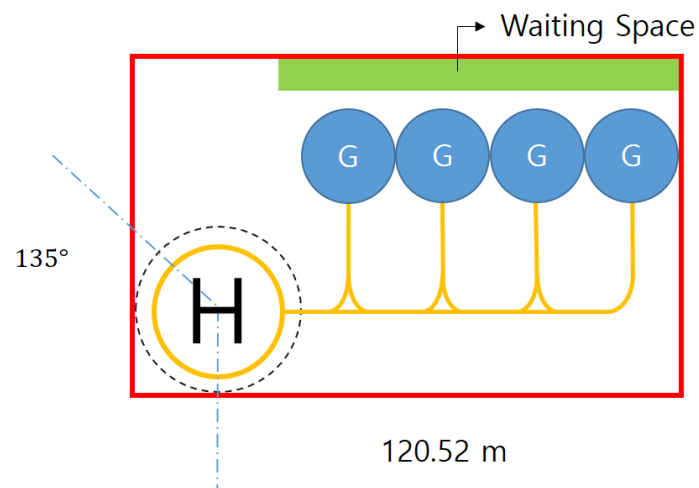


Figure 14. Example of pier topology that complies with the EASA's new regulations.

3. Application to Gimpo Airport

3.1. Size of Gimpo Airport First Parking Lot

The Ministry of Land, Infrastructure, and Transport of Korea announced a road map to utilize airport control, radar, and navigation safety facilities considering the utilization of existing air traffic infrastructure such as at Incheon Airport and Gimpo Airport in Korea. Since vertiports in the airport have the advantage of utilizing the airport's professional manpower and infrastructure in case of emergency and the initial market for UAM is air ambulances and airport shuttles, this study analyzed three types of layouts for Gimpo Airport. The dimensions were calculated using the distance measurement function of Naver Map [20] for analysis, and the previously determined sizes of the vertiport components were used. The parking space was measured for the current parking space at Gimpo Airport's current parking lot and the expanded parking space including the surrounding vacant lot. The FAA's on-airport location of a FATO was reviewed because it is a vertiport to be installed close to the airport runway. The distance between the runway and the center of the FATO requires a minimum separation of 300 ft (91 m) for aircraft weighing less than 12,500 pounds (5670 kg) [14]. The distance between the space considered and the runway is more than 700 m, so it satisfies the requirements.

In this study, a single floor parking space was used. The Korea Airports Corporation presents a double-decker vertihub as shown in Figure 15, and each floor can share aircraft with the others through an elevator.



Figure 15. Gimpo Airport vertihub design of the Korea Airport Corporation [21].

When the vertiport consists of only a single floor, the efficient layout was estimated by classifying the vertiport components into three types in the measured space. The passenger waiting space was considered as an additional component, and for efficient aircraft turnover, a constraint was given to connect at least two gates per one TLOF pad to the remaining space except for the passenger waiting area. Since there is an airport runway in the southwest as shown in Figure 16, the TLOF pad was placed to take off and land except in the southwest direction.

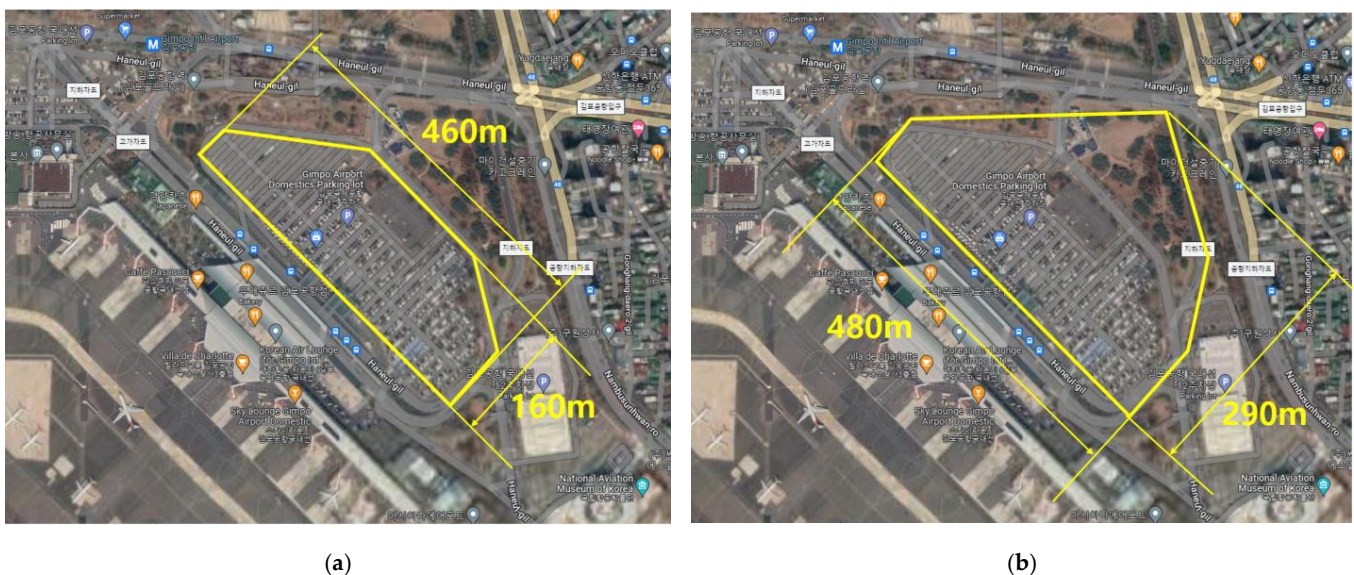


Figure 16. Two topologies for the Gimpo Airport parking lot: (a) current parking space; (b) expanded parking space.

3.2. Three Types of Topology

3.2.1. Linear Topology

In the linear topology, several TLOF pads and gates are arranged in a line. In the absence of a gate, the TLOF pad takes over the role of a gate, so the aircraft turnaround

is performed on the TLOF pad. The linear topology is arranged to support simultaneous operation so that the aircraft operating interval is short, which is useful when it is installed in a narrow and long space [22]. If the space width is large enough, the TLOF pad and gate are installed in a line, which enables simple and fast operation. For the linear topology of the Gimpo Airport parking lot, two layouts were considered, as shown in Figures 17 and 18, that respectively comply with the FAA’s and EASA’s new regulations, and the components of the TLOF pad, gate, and taxiway including the passenger waiting area were included.

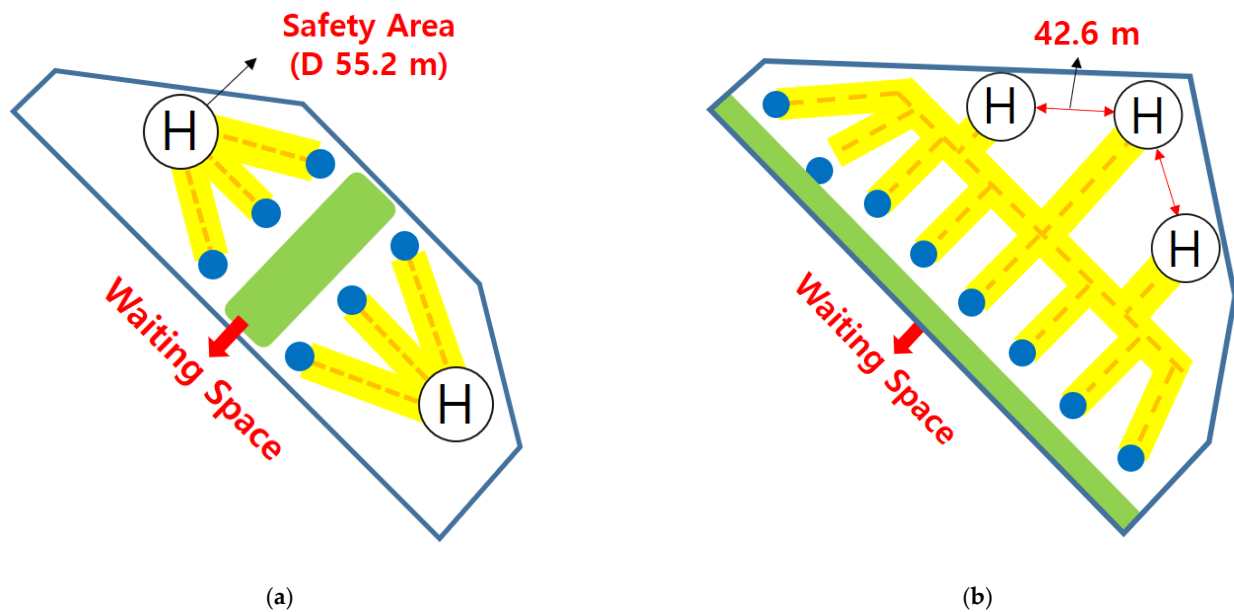


Figure 17. Linear topologies for the Gimpo Airport parking lot that comply with the FAA’s new regulations: (a) current parking space; (b) expanded parking space.

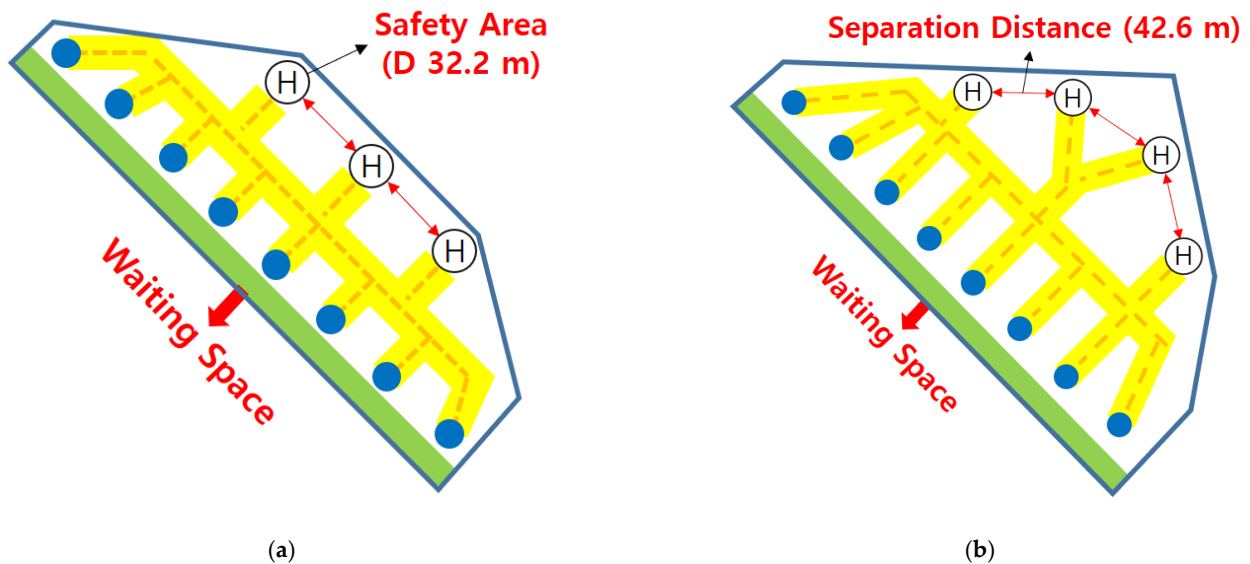


Figure 18. Linear topologies for the Gimpo Airport parking lot that comply with the EASA’s new regulations: (a) current parking space; (b) expanded parking space.

3.2.2. Satellite Topology

A satellite topology has one or more TLOF pads connected to a gate distributed on a circumference of the TLOF pad. In this layout, gates below the flight path cannot be used and are suitable for installation on rooftops and grid-type districts of cities and suburb square spaces [22]. As shown in Figures 19 and 20, the satellite topology can have a

relatively large number of gates per TLOF pad compared to the linear topology, and the aircraft throughput in the TLOF pad is high because the guidance distance is shorter than that of the pier topology.

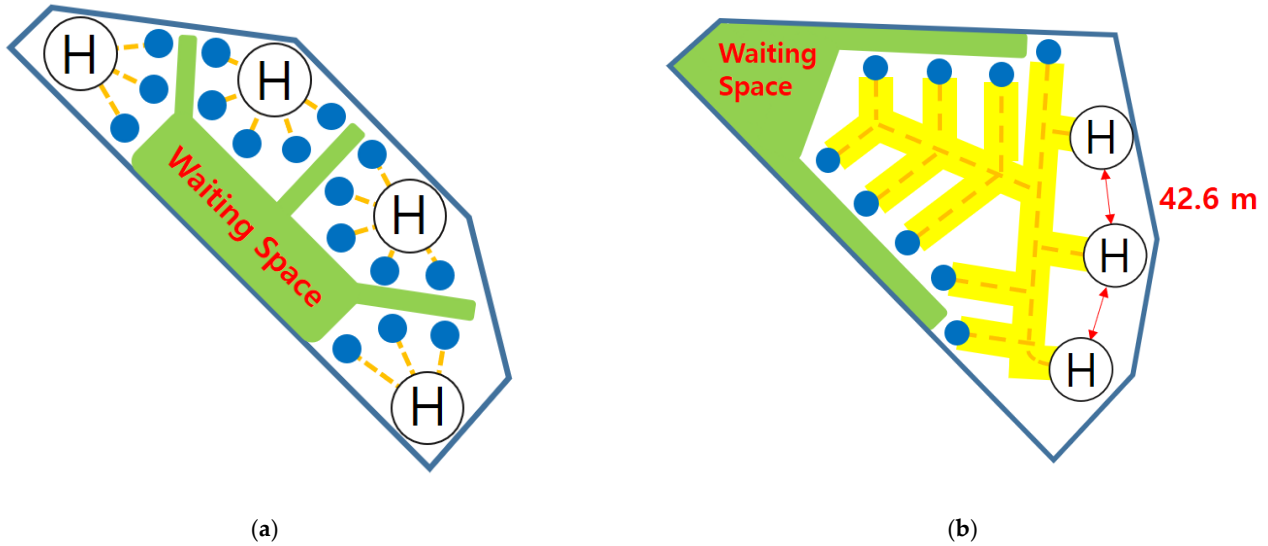


Figure 19. Satellite topologies for the Gimpo Airport parking lot that comply with the FAA’s new regulations: (a) current parking space; (b) expanded parking space.

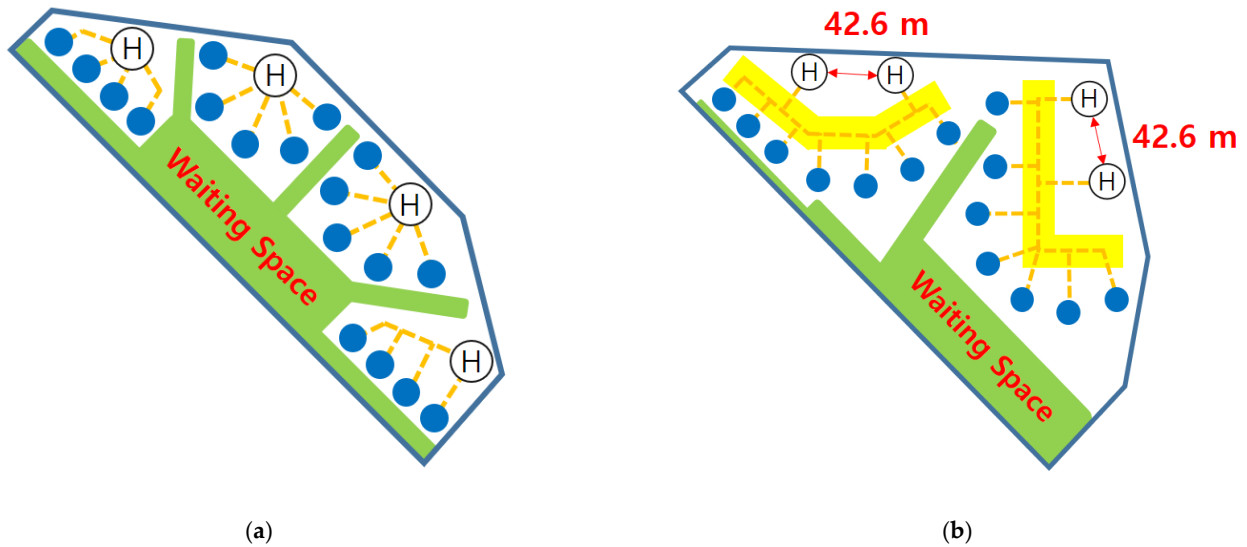


Figure 20. Satellite topologies for the Gimpo Airport parking lot that comply with the EASA’s new regulations: (a) current parking space; (b) expanded parking space.

3.2.3. Pier Topology

The pier topology is a layout in which aircraft can be moved through a long gate aisle. Since the pier topology can accommodate more gates and aircraft than the satellite topology, it can be used to deploy multiple aircraft and to shorten embarkation and disembarkation times [22]. As shown in Figures 21 and 22, since the TLOF pad and the gate area are clearly separated, congestion of the vertiport is low.

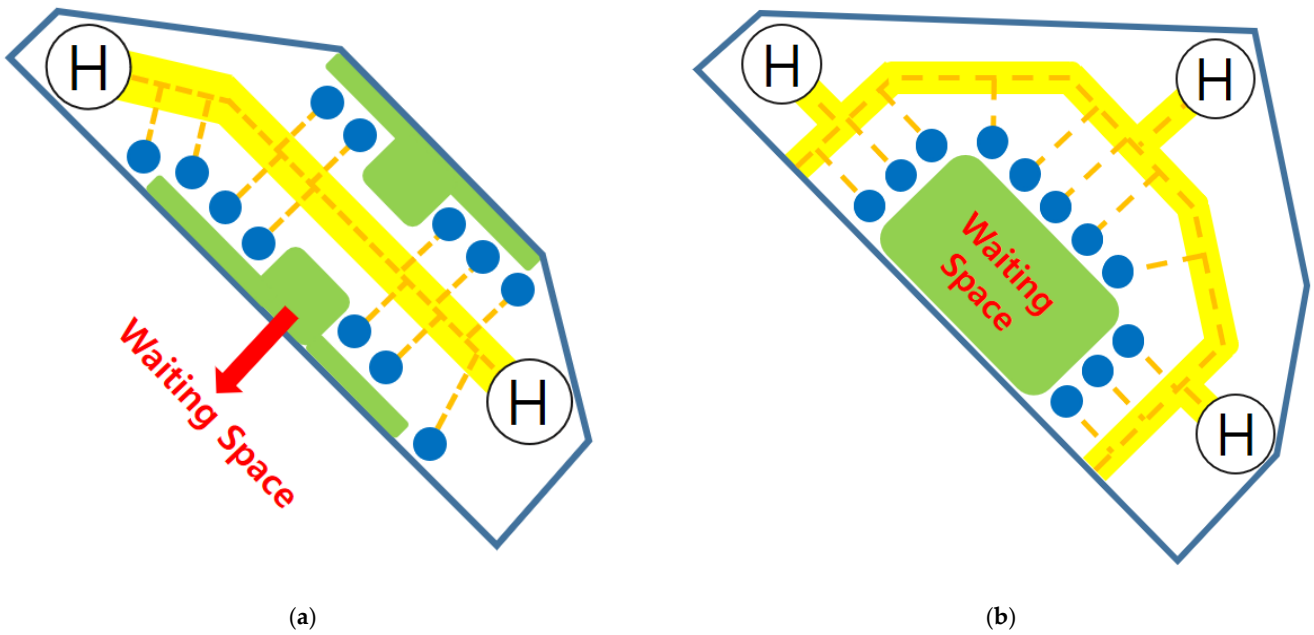


Figure 21. Pier topologies for the Gimpo Airport parking lot that comply with the FAA’s new regulations: (a) current parking space; (b) expanded parking space.

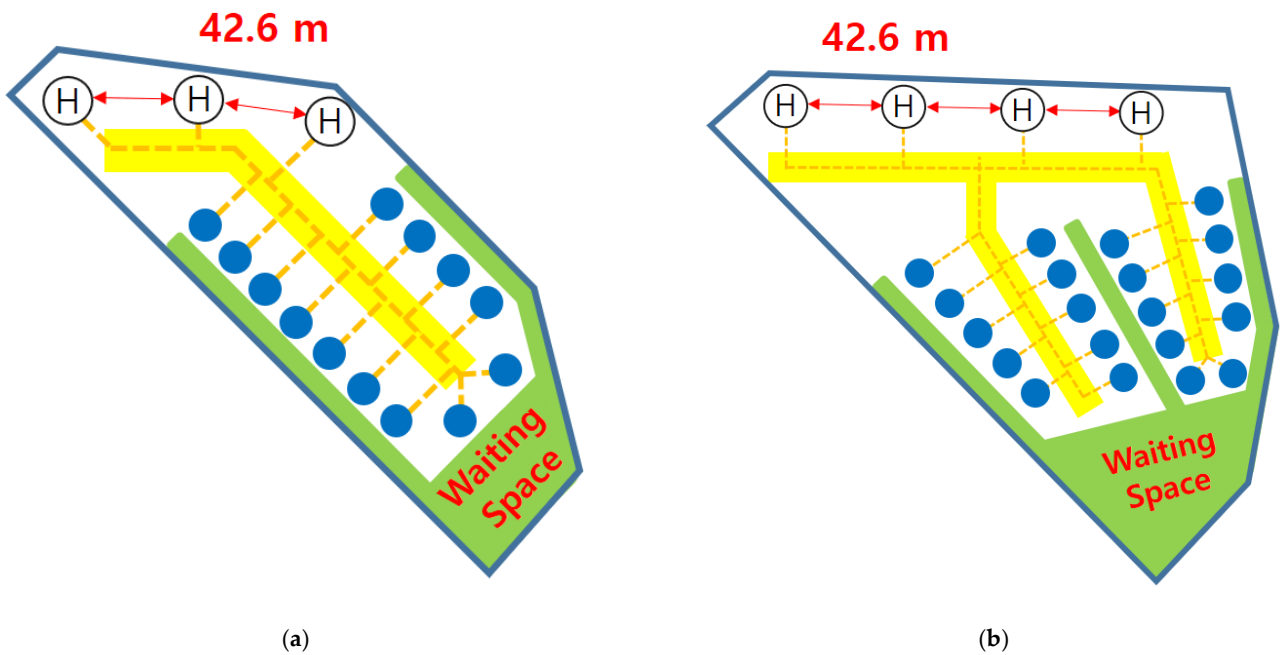


Figure 22. Pier topologies for the Gimpo Airport parking lot that comply with the EASA’s new regulations: (a) current parking space; (b) expanded parking space.

4. Capacity Analysis for Each Topology

4.1. Theoretical Background

For UAM operation, a vertiport will be newly built in a limited space in a downtown area or integrated with existing infrastructure. Therefore, it is necessary to consider a layout that can operate as many aircraft as possible in a limited space, so we compared the three layouts reviewed in the previous section under the same conditions to evaluate capacity.

The operating procedure of the aircraft in the vertiport is shown in Figure 23. While the simultaneous operating distance of AC 150/5390-2C was applied, the capacity analysis code was written with the assumption that the vertiport is empty at $t = 0$. To accommodate

the maximum number of aircraft, arrival is prioritized over departure in the TLOF pad. For the safe operation of the vertiport, there can be only one aircraft at the node where the TLOF pad and gate are connected. For example, when an aircraft is arriving at a vertiport with one TLOF pad, step ⑤ cannot be performed.

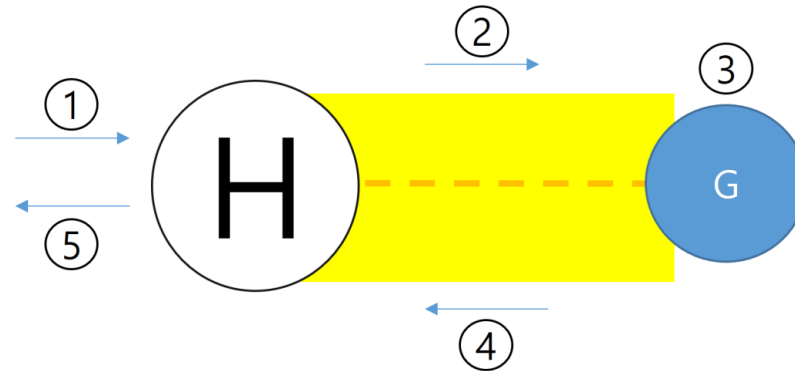


Figure 23. Operation process on a vertiport. ① is arrival, ② is taxiing to gate, ③ is gate, ④ is taxiing to TLOF pad, ⑤ is departure.

Figure 24 shows the possible departure/arrival integer pairs. The section ① is the number of times the vertiport can accommodate the arrival of aircraft and is created to be as much as the number of aircraft arrivals that fill the gate in the initial state. Sections ② and ③ are linear by giving priority to arrival where departure or arrival is possible. Sections ④ and ⑤ are free-operation sections, and in section ④, departures can occur without reducing the number of arrivals. The free-operation section may vary depending on the number of prearranged aircraft, arrival time, departure time, turnaround time, etc. [7]. Section ⑥ is a section in which the sum of feasible departures and arrivals in the vertiport is maximum and can be created as a single point or as a line by decreasing arrivals and increasing departures. Therefore, an integer pair in this section means the maximum capacity of the vertiport. Section ⑦ is created when there is an aircraft prepared in advance, i.e., when an arrival is blocked and a departure occurs.

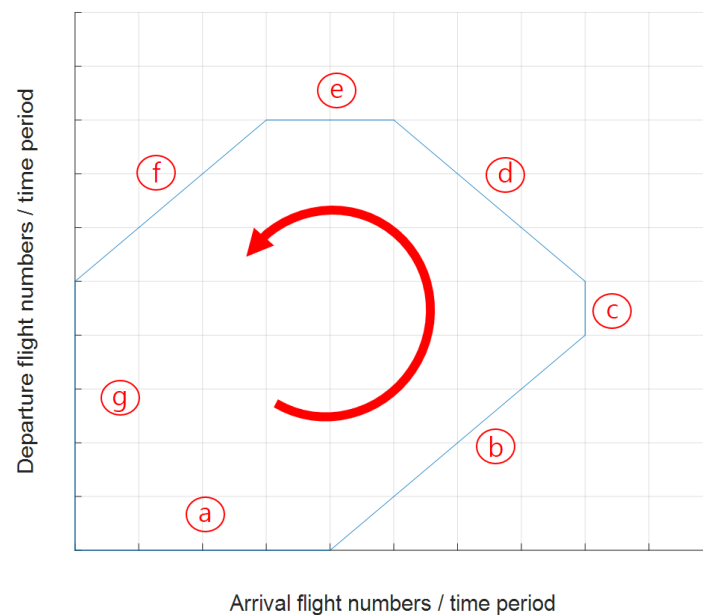


Figure 24. Integer pairs of departures and arrivals: section ① is the number of accommodated aircraft when the vertiport is empty; ② and ③ are the priority arrival sections; ④ and ⑤ are the free-operation sections; section ⑥ has the maximum of feasible departure and arrival; and section ⑦ is the section with prepared departure aircraft.

In this study, the capacity was analyzed using Matlab and the departure/arrival integer pair was expressed while satisfying Equations (1)–(4) for n gates and time t . Figure 25 shows the operation procedure of each aircraft at one to four gates of a vertiport with one TLOF pad and four gates.

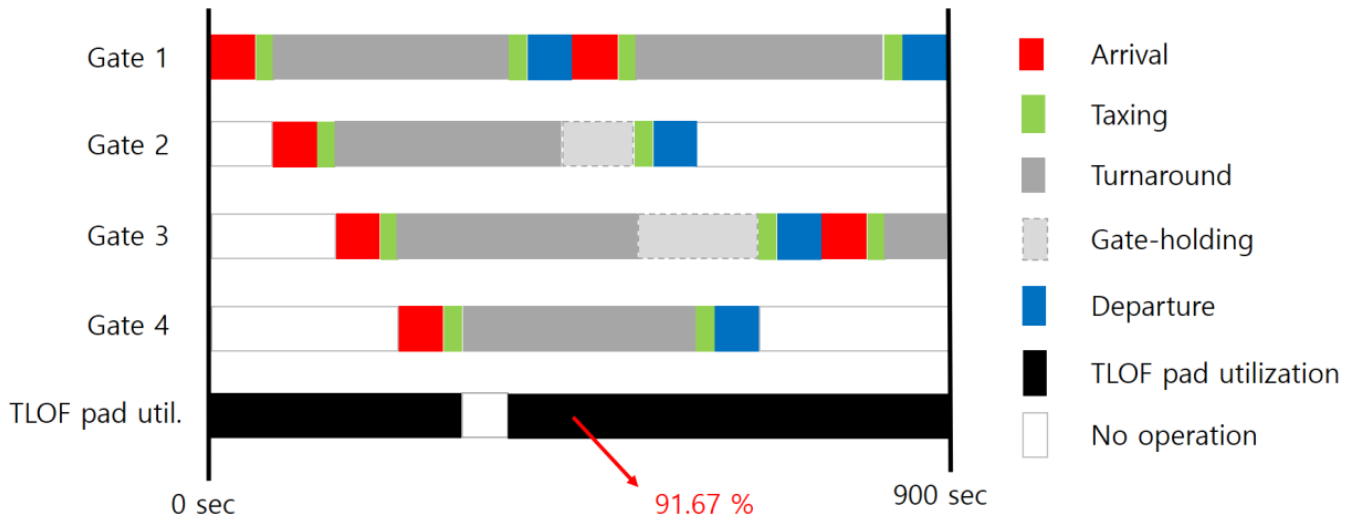


Figure 25. TLOF pad utilization rate (one TLOF pad, four gates).

The TLOF pad utilization rate is the time ratio for arrival, taxi-in, taxi-out, and departure in the total time as shown in Figure 25. The gate utilization rate is calculated as the average of the time ratio of the taxi-in, taxi-out, and turnaround time on each gate in the total time, and then calculated again as an average for all gates when the capacity reaches the max-throughput in Equation (5). In the case of gate utilization, even if the turnaround of the aircraft is completed, there could be a waiting time for departure that is due to priority on arrival, and this congestion time is also counted. The gate holding time increases when the equal sign is satisfied in Equation (4) and is calculated using Equation (6). Table 3 summarizes the variables used in the equations.

$$\sum_{n=1}^{N_{tlof}} N_{arr}(t, n) - \sum_{n=1}^{N_{tlof}} N_{dep}(t, n) \geq 0 \forall t, n \tag{1}$$

$$\sum_{n=1}^{N_{tlof}} (C_{tlof} + C_{taxi}) = N_{tlof} \forall t \tag{2}$$

$$\sum_{n=1}^{N_{gate}} (C_{gate} + C_{taxi}) = N_{gate} \forall t \tag{3}$$

$$N_{trd}(t, n) \leq \frac{N_{arr}(t, n) + N_{taxi}(t)}{2} \forall t \tag{4}$$

$$t_{g-h}(t, n) = \frac{t_{trd} \cdot \sum_{n=1}^{N_{gate}} (N_{trd}(t, n))}{N_{gate} \cdot T} \forall t, n \tag{5}$$

$$\frac{\sum_{n=1}^{N_{gate}} (t_{g-h}(t, n))}{N_{gate} \cdot T} \forall t, n \tag{6}$$

where $N_{arr}(t, n)$, $N_{dep}(t, n)$, $C_{tlof}(t, n)$, $C_{gate}(t, n)$, C_{taxi} , $N_{trd}(t, n)$, $N_{gate}(t, n)$ are positive integers.

Table 3. Variables for capacity determination algorithm.

| Variable | Meaning |
|-----------------|--|
| C_{tlof} | Capacity of TLOF pads |
| C_{gate} | Capacity of gates |
| C_{taxi} | Capacity of taxiways |
| N_{tlof} | Number of TLOF pads of vertiport |
| N_{gate} | Number of gates of vertiport |
| $N_{arr}(t, n)$ | Number of completed arrivals at n -th gate |
| $N_{dep}(t, n)$ | Number of completed departures at n -th gate |
| $N_{taxi}(t)$ | Number of completed taxing operation |
| $t_{trd}(t, n)$ | Turnaround time at n -th gate |
| $t_{g-h}(t, n)$ | Gate holding time at n -th gate |
| T | Operation time |

The dimensions and slope of obstacle limitation surfaces for all visual FATOs were summarized in Table 4.

Table 4. Dimensions and slope of obstacle limitation surfaces for all visual FATOs [15].

| Components | Slope Design Categories | | |
|-----------------------------|-------------------------|----------------------|----------------------|
| | Width of Safety Area | Width of Safety Area | Width of Safety Area |
| Length of inner edge | | | |
| Length | 3386 m | 245 m | 1220 m |
| Slope | 4.5% (1:22.2) | 8% (1:12.5) | 12.5% (1:8) |
| Transitional Surface Slope | 50% (1:2) | 50% (1:2) | 50% (1:2) |
| Transitional Surface Height | 45 m | 45 m | 45 m |

4.2. Application to Three Kinds of Topologies

The number of arrivals and departures of aircraft is the most important factor for analyzing throughput of a vertiport. Therefore, TLOF pad utilization is prior criteria for an efficient layout, and gate utilization should be considered when similar TLOF pad utilizations are given. Although the taxiways connecting the TLOF pad and the gate have different lengths, in this study, all taxiing times were assumed to be 15 s. In addition, the capacity of each vertiport was calculated for 15 min initially, and converted for one hour of operation to have the highest efficiency so that the analysis data can be easily interpreted. Segment time spending for one TLOF pad and four gates was explained in Table 5.

Table 5. Segment time spending (one TLOF pad, four gates).

| Time Spending | Time (s) |
|---------------|----------|
| Arrival | 60 |
| Taxi-in | 15 |
| Turnaround | 300 |
| Taxi-out | 15 |
| Departure | 60 |

An example of a vertiport composed of one TLOF pad and four gates with an empty vertiport was analyzed as shown in Figure 26. This analysis shows the maximum capacity that performs the (7, 4) arrivals and departures or the (6, 5) arrivals and departures by

applying the time duration of each section in Table 5 during a 15 min operation time. ○ stands for arrival, × stands for departure, □ stands for free-arrival, and * stands for max-throughput. If there is no *, the last generated × becomes the unique max-throughput.

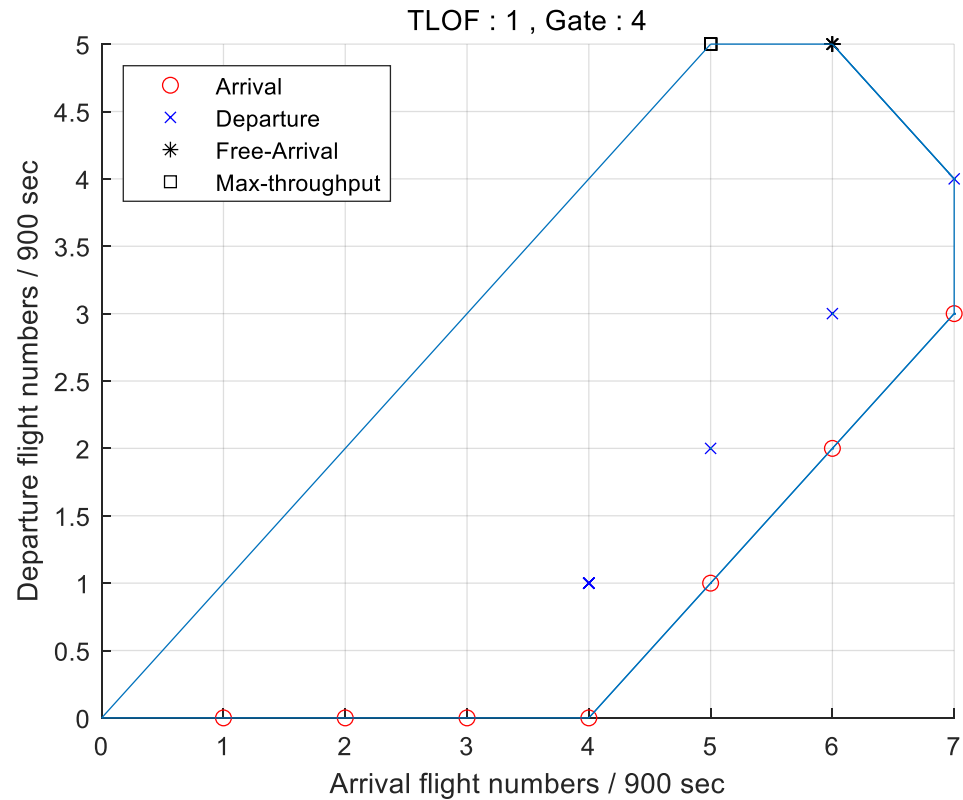


Figure 26. Example of vertiport capacity (one TLOF pad, four gates).

For the S-A1 capable of carrying four passengers, this vertiport can accommodate 20 passengers during its 15 min operation time because it can perform five departures after six aircraft arrivals for max-throughput so it can accommodate 80 passengers per hour. Table 6 summarizes the results of this analysis.

Table 6. Analysis results of vertiport consisting of one TLOF and four gates.

| Number of TLOF Pads | 1 |
|---------------------------------------|------|
| Number of gates | 4 |
| TLOF pad utilization (%) | 91.7 |
| Gate utilization (%) | 61.9 |
| Gate holding (%) | 8.3 |
| Maximum number of passengers per hour | 80 |

4.3. Application to Gimpo Airport

For the current parking space of Gimpo Airport assumed as having a single story, the capacities of each linear, satellite, and pier topologies are shown in Figures 27–32, respectively, by applying the regulations of the FAA and EASA. The utilization and capacity for the satellite topology are calculated as the average of operating one TLOF pad and two gates and one TLOF pad and four gates because TLOF pads cannot share a gate.

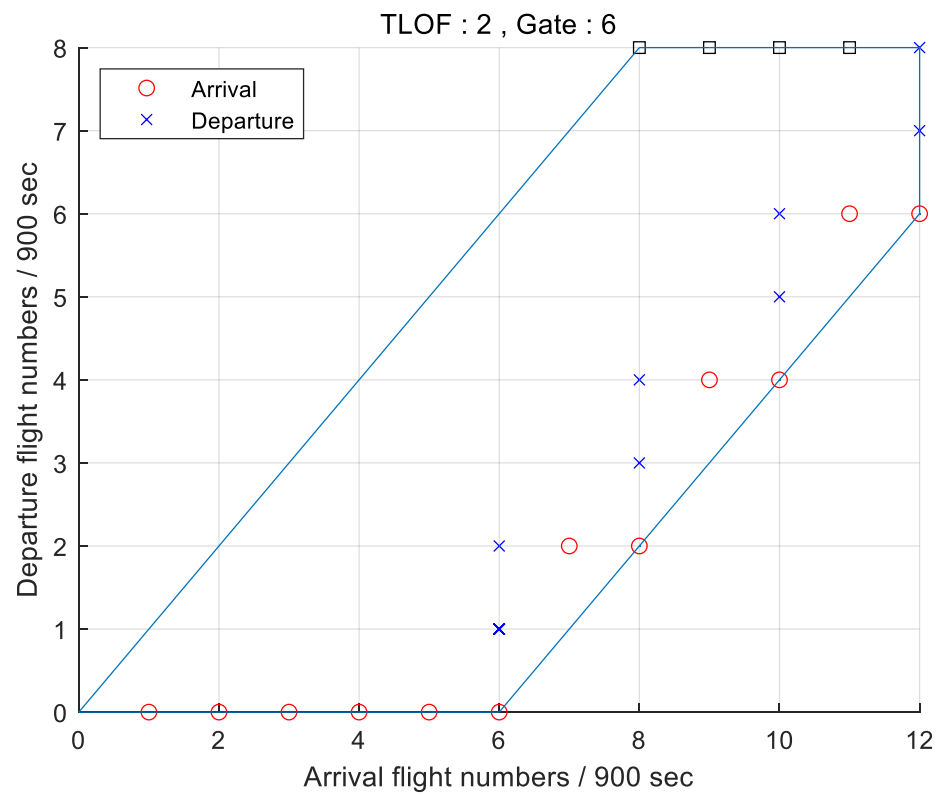


Figure 27. The linear topology capacity of the current Gimpo Airport parking lot that complies with the FAA’s new regulations.

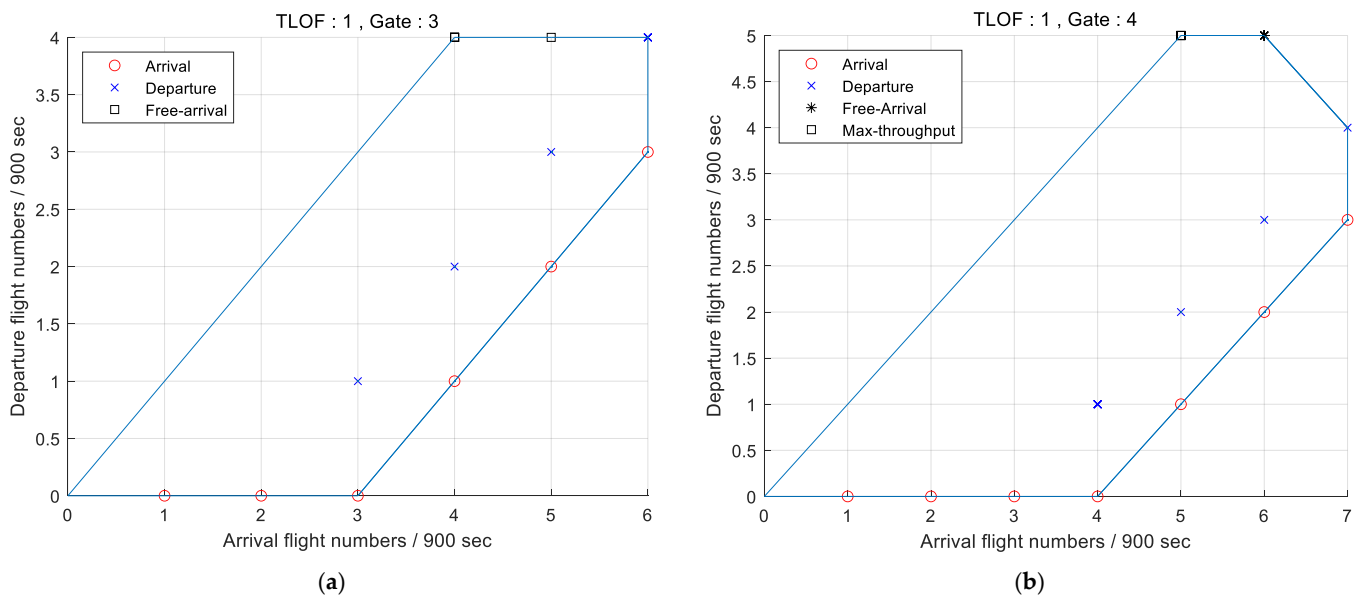


Figure 28. The satellite topology capacity of the current Gimpo Airport parking lot that complies with the FAA’s new regulations: (a) 1 TLOF, 3 Gates; (b) 1 TLOF, 4 Gates.

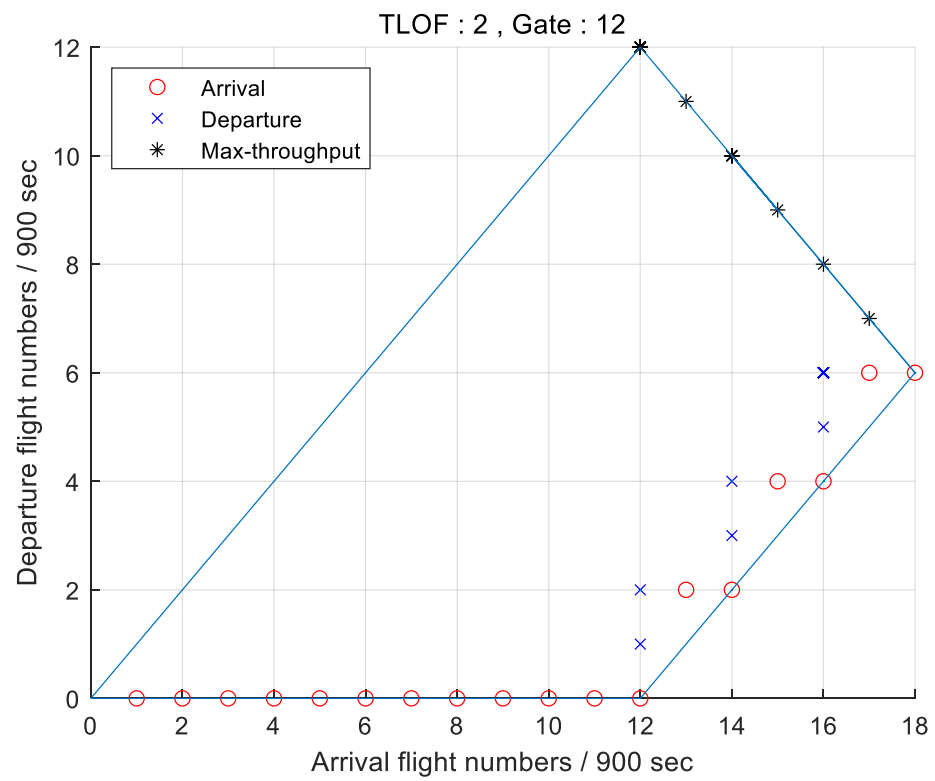


Figure 29. The pier topology capacity of the current Gimpo Airport parking lot that complies with the FAA's new regulations.

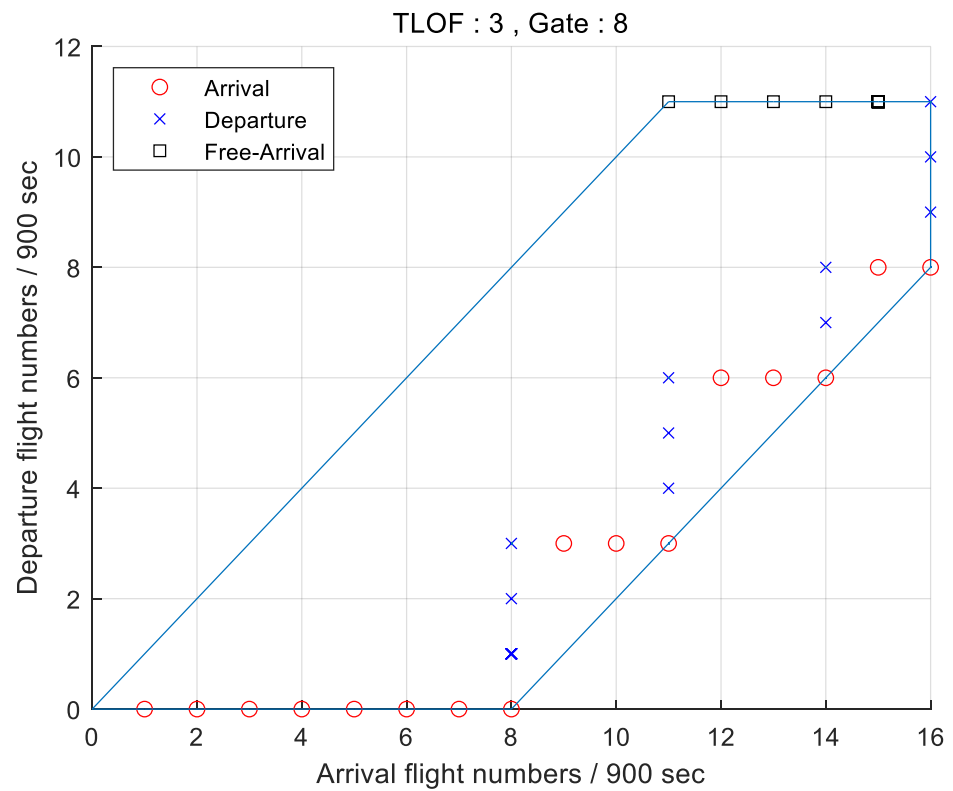


Figure 30. Capacity of a linear topology for the current Gimpo Airport parking lot that complies with the EASA's new regulations.

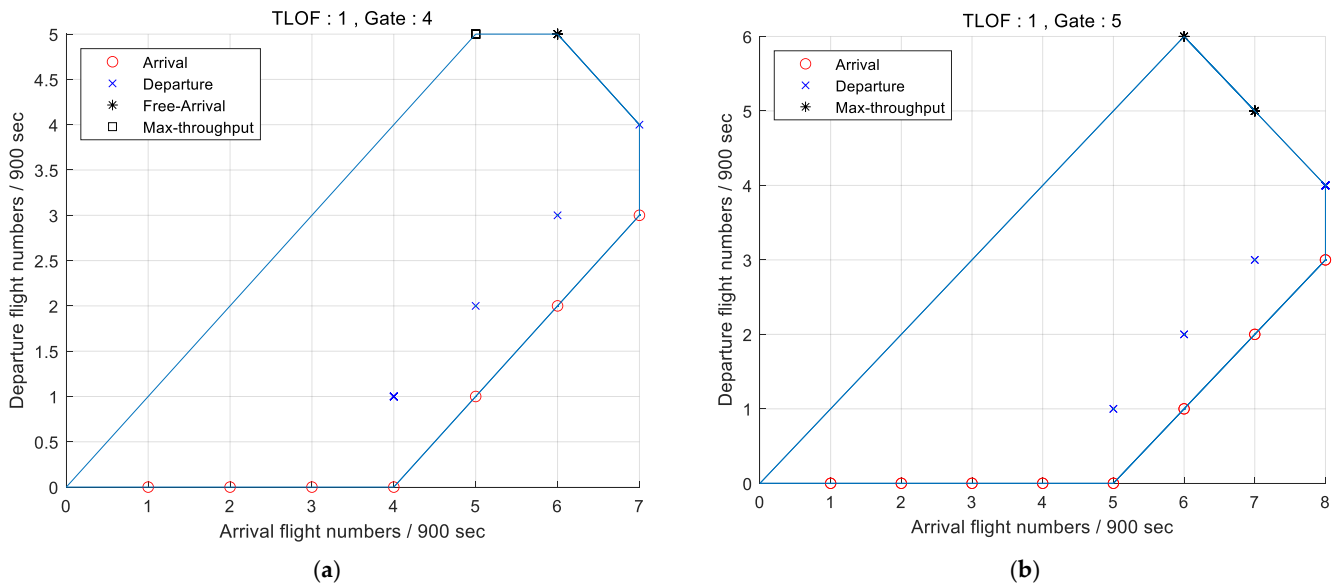


Figure 31. Capacity of a satellite topology for the current Gimpo Airport parking lot that complies with the EASA’s new regulations: (a) 1 TLOF, 4 Gates; (b) 1 TLOF, 5 Gates.

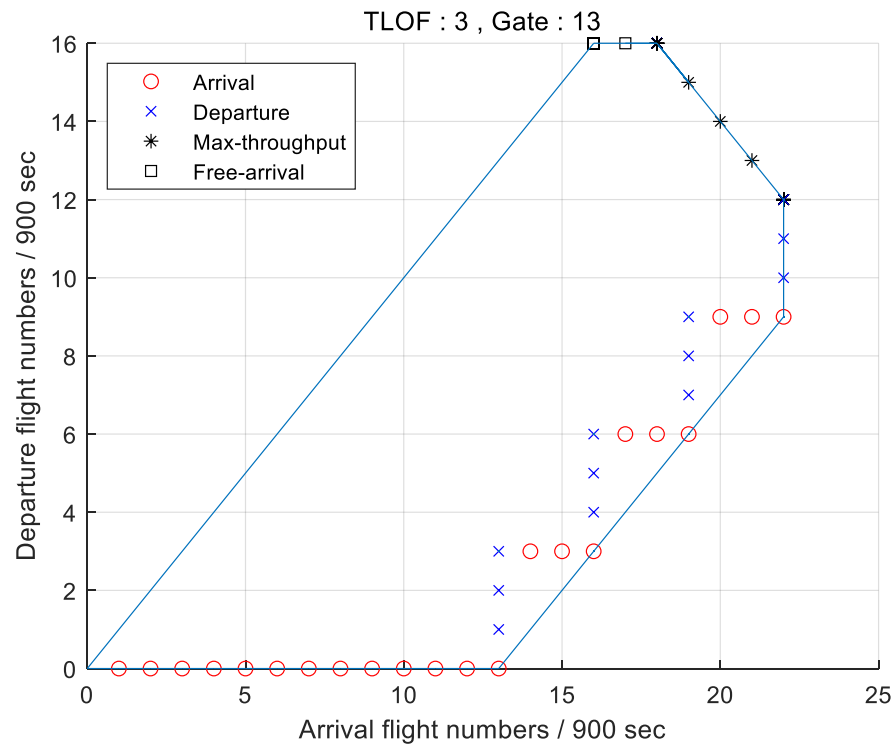


Figure 32. Capacity of a pier topology for the current Gimpo Airport parking lot that complies with the EASA’s new regulations.

As shown in Table 7, the pier topology with 2 TLOF pads and 12 gates shows the best efficiency with 100% TLOF pad utilization. In addition, the arrival/departure pair (12, 12) with the most departures can be selected from the max-throughput because departures are important as a criterion for determining the number of accommodated passengers. Assuming that this vertiport operates an eVTOL aircraft carrying 4 passengers, excluding the pilot, it can carry 48 passengers in 15 min, through 48 arrivals and 48 departures, and can accommodate a total of 192 passengers per hour if 1 h operation time is used instead of 15 min.

Table 7. Results of each topology for the current Gimpo parking lot space that complies with the FAA's new regulations.

| Topology | Number of TLOF Pads | Number of Gates | TLOF Pad Utilization (%) | Gate Utilization (%) |
|-----------|---------------------|-----------------|--------------------------|----------------------|
| Linear | 2 | 6 | 83.3 | 72.4 |
| Satellite | 4 | 16 | 91.7 | 43.4 |
| Pier | 2 | 12 | 100 | 55.5 |

As shown in Table 8, the satellite topology that complies with the EASA's new regulations shows the best efficiency with 95.8% TLOF pad utilization. In addition, the arrival/departure pair (18, 16) with the most departures can be selected from the max-throughput because departures are important as a criterion for determining the number of accommodated passengers. Assuming that this vertiport operates an eVTOL aircraft carrying 4 passengers, excluding the pilot, it can accommodate a total of 256 passengers per hour.

Table 8. Results of each topology for the current Gimpo parking lot space that complies with the EASA's new regulations.

| Topology | Number of TLOF Pads | Number of Gates | TLOF Pad Utilization (%) | Gate Utilization (%) |
|-----------|---------------------|-----------------|--------------------------|----------------------|
| Linear | 3 | 8 | 75 | 53.6 |
| Satellite | 4 | 18 | 95.8 | 43.2 |
| Pier | 3 | 13 | 94.4 | 53.5 |

In the same way, the capacities of the linear, satellite, and pier topologies for the expanded space of Gimpo Airport are shown in Figures 33–38, respectively, by applying the regulations of the FAA and EASA. As shown in Table 9, the satellite topology with 3 TLOF pads and 11 gates shows the best efficiency of 88.9% TLOF pad utilization. For (18, 14) arrival/departure pairs with the maximum departures, assuming an eVTOL carrying 4 passengers, it can carry 56 passengers in 15 min, and can accommodate a total of 272 passengers with 72 arrivals and 68 departures per hour if 1 h operation time is used instead of 15 min. As shown in Table 10, the pier topology that complies with the EASA's new regulations shows the best efficiency with 100% TLOF pad utilization. In addition, the arrival/departure pair (24, 24) with the most departures can be selected from the max-throughput because departures are important as a criterion for determining the number of accommodated passengers. Assuming that this vertiport operates an eVTOL aircraft carrying 4 passengers, excluding the pilot, it can accommodate a total of 384 passengers per hour.

Table 9. Results of each topology for the expanded Gimpo parking lot space that complies with the FAA's new regulations.

| Topology | Number of TLOF Pads | Number of Gates | TLOF Pad Utilization (%) | Gate Utilization (%) |
|-----------|---------------------|-----------------|--------------------------|----------------------|
| Linear | 3 | 8 | 75 | 70.2 |
| Satellite | 3 | 9 | 83.3 | 69.4 |
| Pier | 3 | 11 | 88.9 | 54.2 |

Table 10. Results of each topology for the expanded Gimpo parking lot space that complies with the EASA’s new regulations.

| Topology | Number of TLOF Pads | Number of Gates | TLOF Pad Utilization (%) | Gate Utilization (%) |
|-----------|---------------------|-----------------|--------------------------|----------------------|
| Linear | 4 | 8 | 58.3 | 54.8 |
| Satellite | 2 | 7 | 87.5 | 52.2 |
| Pier | 4 | 20 | 100 | 57.5 |

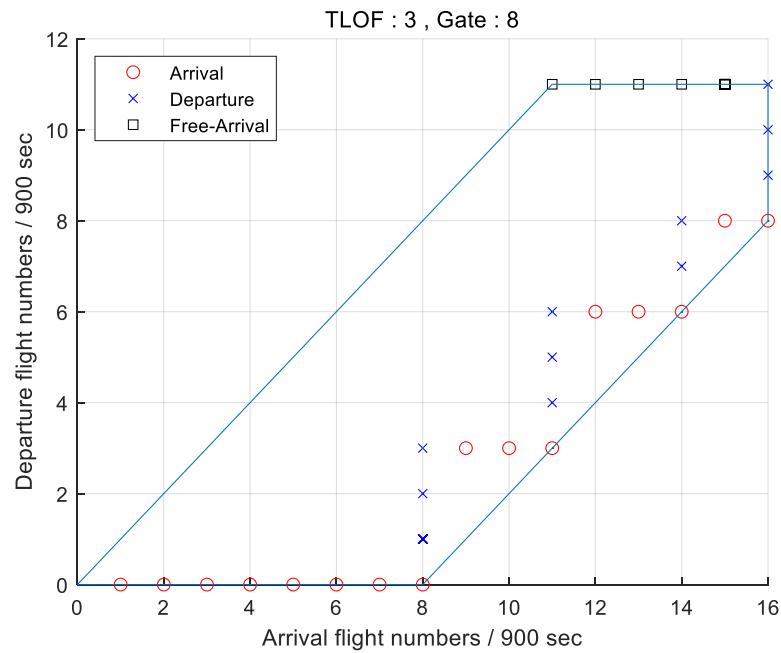


Figure 33. Capacity of a linear topology for Gimpo Airport’s expanded parking lot space that complies with the FAA’s new regulations.

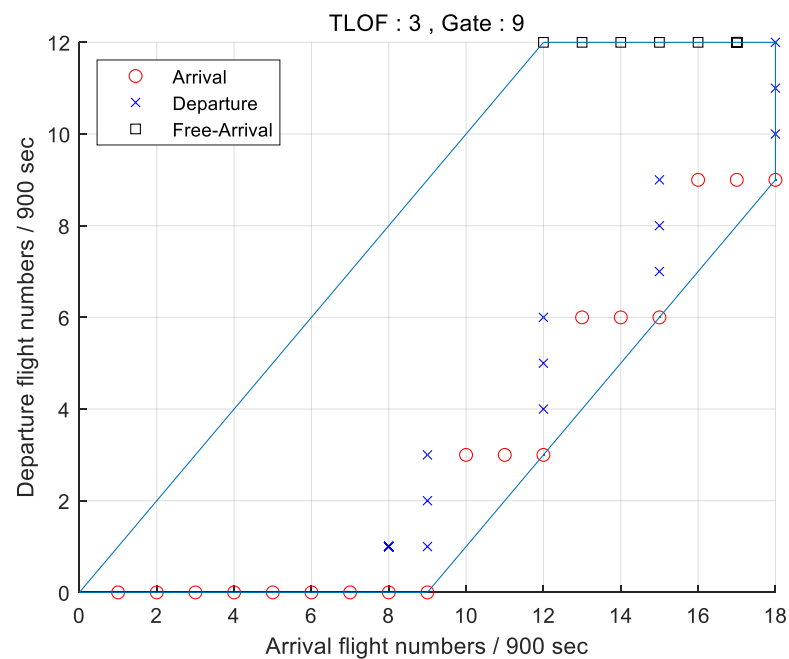


Figure 34. Capacity of a satellite topology for Gimpo Airport’s expanded parking lot space that complies with the FAA’s new regulations.

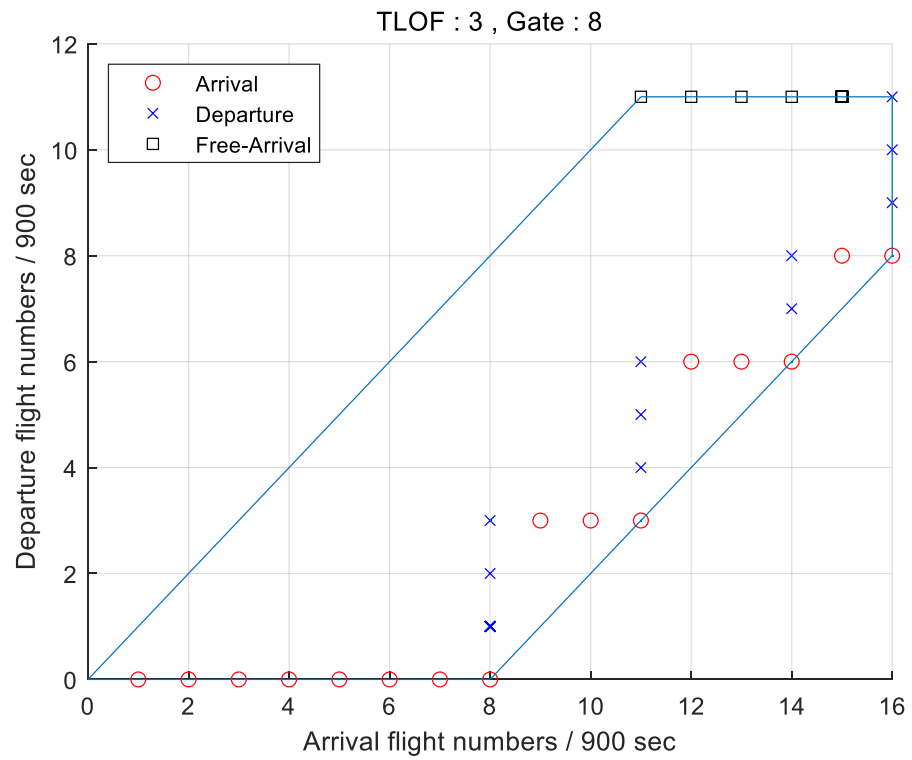


Figure 35. Capacity of a pier topology for Gimpo Airport's expanded parking lot space that complies with the FAA's new regulations.

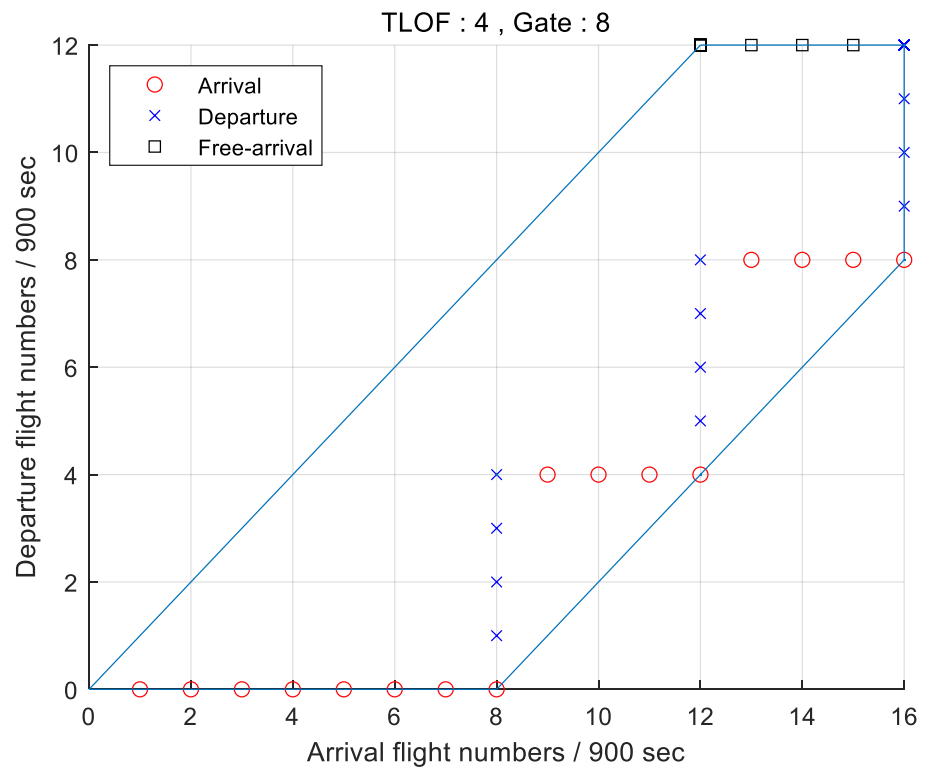


Figure 36. Capacity of a linear topology for the expanded Gimpo Airport parking lot that complies with the EASA's new regulations.

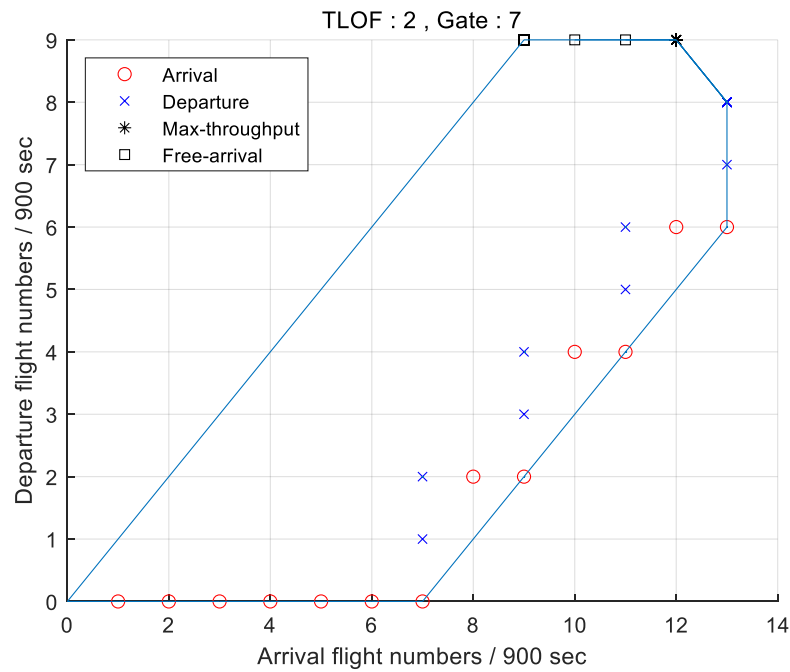


Figure 37. Capacity of a satellite topology for the expanded Gimpo Airport parking lot that complies with the EASA’s new regulations.

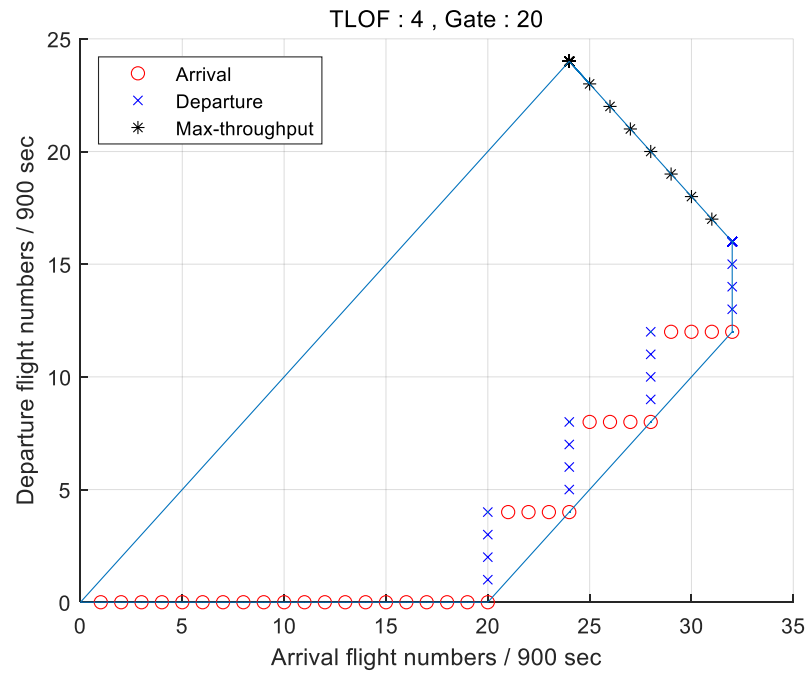


Figure 38. Capacity of a pier topology for the expanded Gimpo Airport parking lot that complies with the EASA’s new regulations.

As a result, if the FAA’s new regulations are applied, the most efficient vertiport layout for UAM operation in the Gimpo Airport parking lot is a pier topology consisting of two TLOF pads and 12 gates for the current parking space and the pier topology consisting of three TLOF pads and 11 gates for the expanded parking space. If the EASA’s new regulations are applied, the most efficient layouts are the satellite topology consisting of 4 TLOF pads and 18 gates for the current parking space and pier topology consisting of 4 TLOF pads and 20 gates for the expanded parking space.

The approach/departure surface that comply with the EASA’s new regulations is applied to Gimpo Airport as shown in Figures 39 and 40. The dimensions of the approach/departure surface at Gimpo Airport is summarized in Table 11.

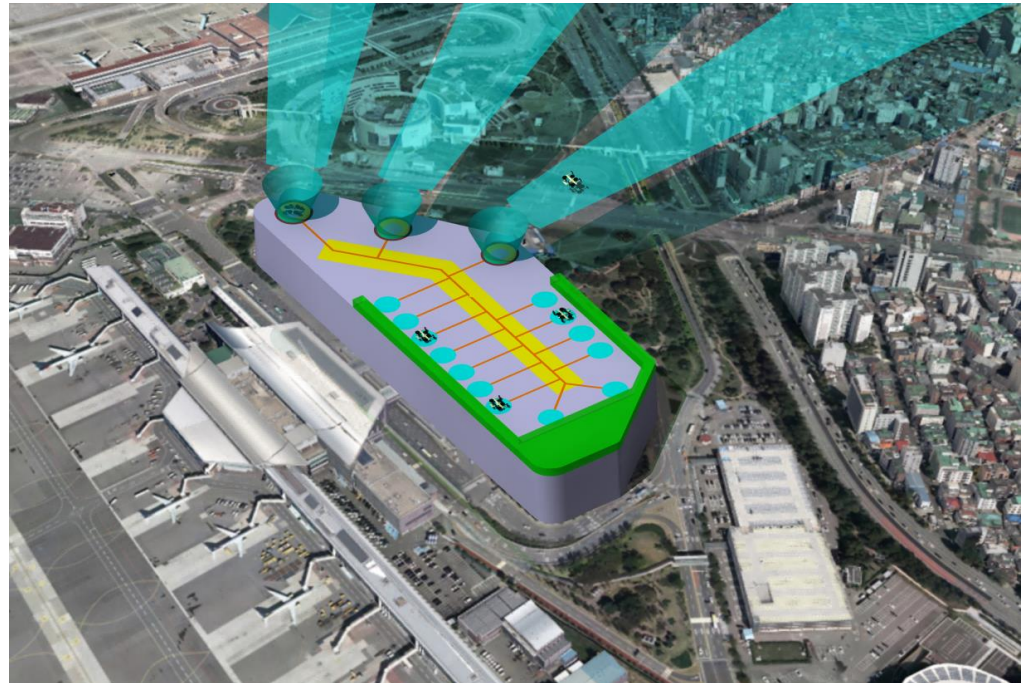


Figure 39. Example of vertiport approach/departure surfaces with the EASA’s regulations for a pier topology at the current Gimpo Airport parking lot.

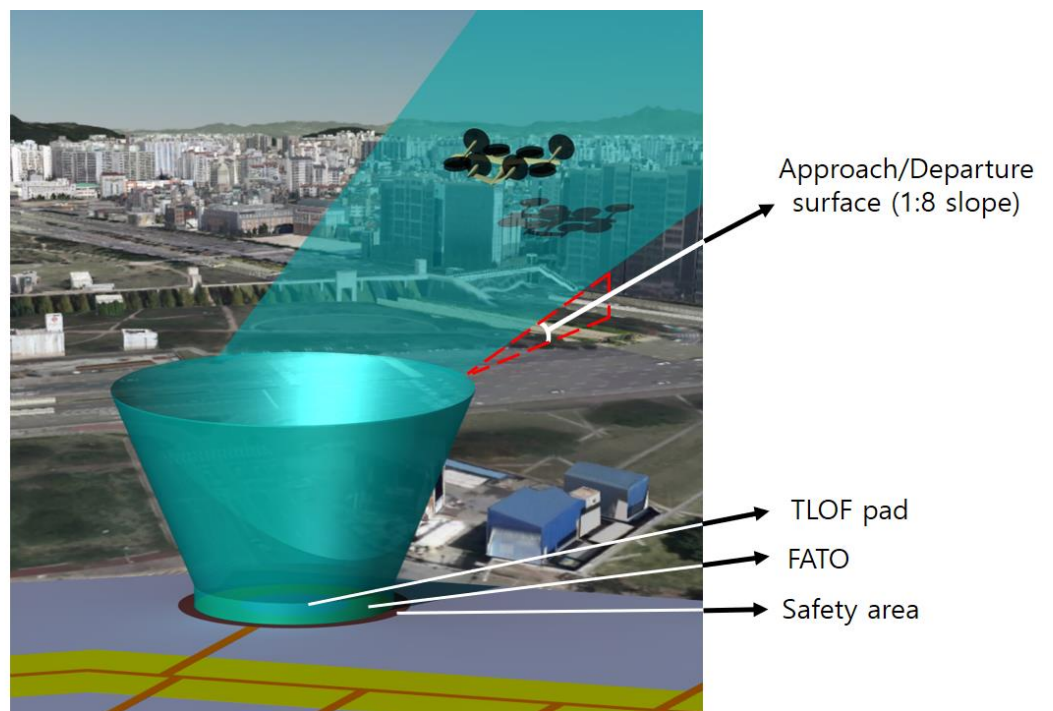


Figure 40. Detail approach/departure surfaces for a pier topology at the current Gimpo Airport parking lot that comply with the EASA’s new regulations.

Table 11. The dimensions of the approach/departure surface for the pier topology at the current Gimpo Airport parking lot that comply with the EASA’s new regulations.

| Sections | Standard | Applied Value |
|----------------------------|------------------|---------------|
| Approach/departure surface | 1:8 (12.5%) | 1:8 (12.5%) |
| TO | Safety area + CD | 50.6 m |
| FATO | $2 \times CD$ | 27.6 m |
| h_1 | - | 3 m |
| h_2 | $\geq h_1$ | 30.5 m |

4.4. Application to the Design Proposed by Korea Airports Corporation

The capacity analysis algorithm was applied to the vertihub in Figure 15 presented by the Korea Airports Corporation. Each floor of this vertihub consists of a total of 5 TLOF pads and 51 gates as shown in Figures 41 and 42, and an aircraft can be moved to another floor through an elevator. The capacity was analyzed by assuming that a double-decker vertihub is the same as a single floor.

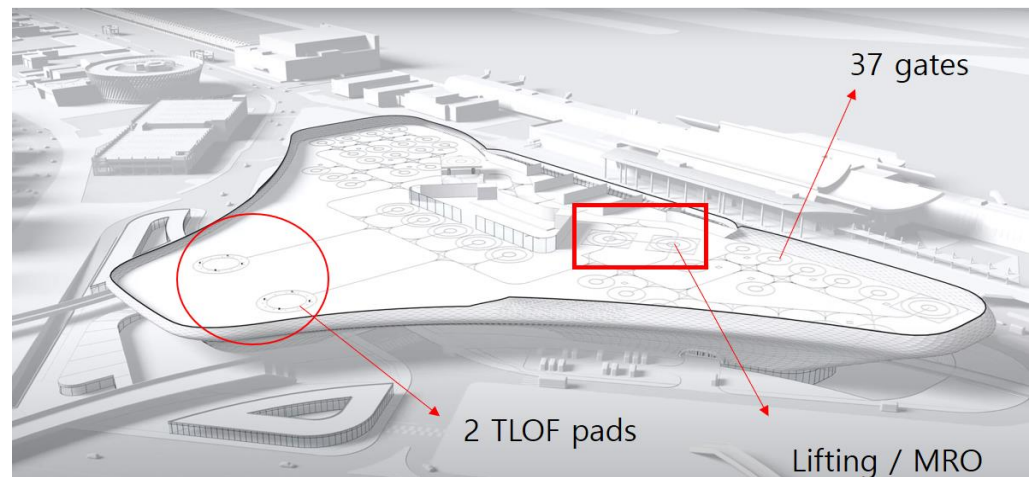


Figure 41. The lower deck design of the Gimpo Airport vertihub [21].

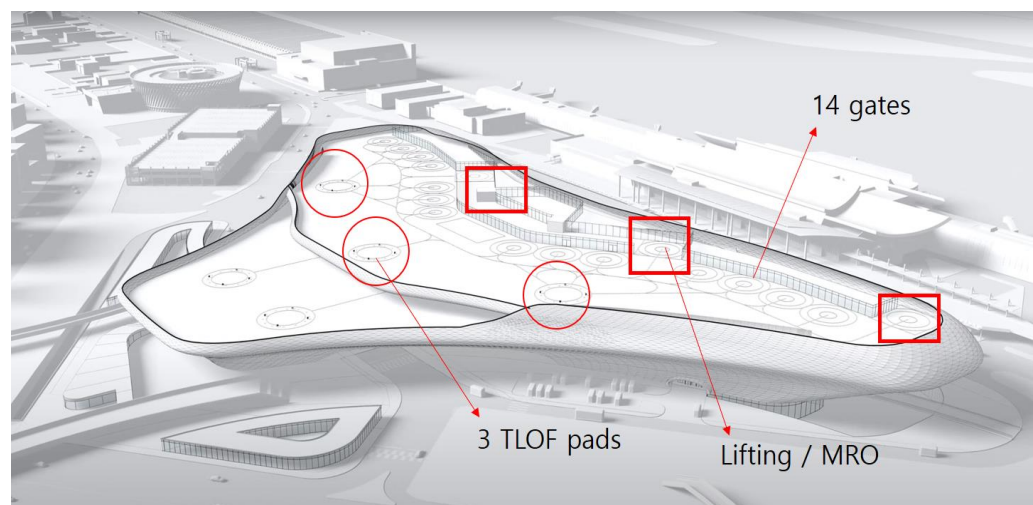


Figure 42. The upper deck design of the Gimpo Airport vertihub [21].

As shown in Figure 43 and Table 12, the total number of passengers who can be accommodated at the Gimpo Airport vertihub is 448 for 15 min operation time. Converting

to one hour of operation time, it can accommodate a total of 472 passengers with 118 arrivals and 118 departures.

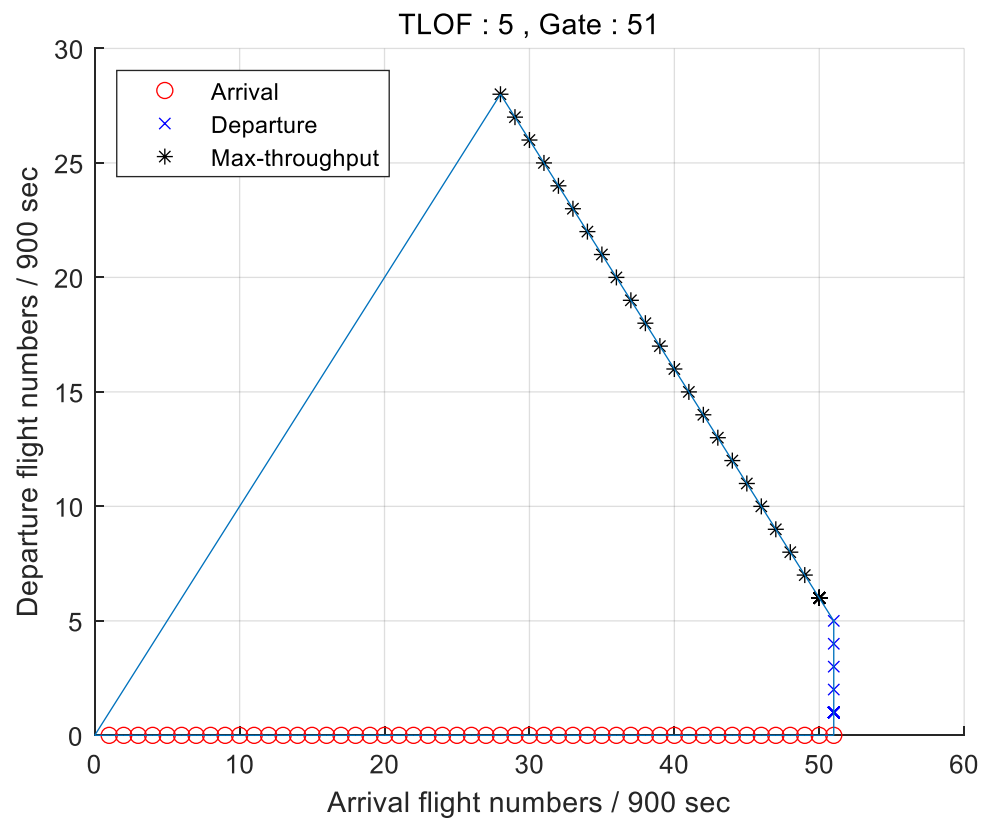


Figure 43. Capacity of the Gimpo Airport vertihub.

Table 12. Analysis results of the vertihub of the Korea Airports Corporation.

| | |
|---------------------------------------|------|
| Number of TLOF Pads | 5 |
| Number of gates | 51 |
| TLOF pad utilization (%) | 93.3 |
| Gate utilization (%) | 41.0 |
| Gate holding (%) | 0.8 |
| Maximum number of passengers per hour | 472 |

The gate size of this vertihub is 18 m in diameter, which is different from this research. The proposed gate sizes and the total number of gates are different because of the size gap between aircraft designated by the Korea Airports Corporation and S-A1.

4.5. Results of Analysis

Figures 44 and 45 show the TLOF pad utilization and the maximum number of passengers per hour for different numbers of TLOF pads and gates. The TLOF pad utilization, which is the standard for the process of selecting an efficient layout, is proportional to the number of passengers. Figure 44 shows that the maximum efficiency can be obtained by using the fewest components when the ratio of TLOF pad to gate is 1:5. Figure 45 proposes the criteria for selecting the number of TLOF pads and gates for the given vertiport space.

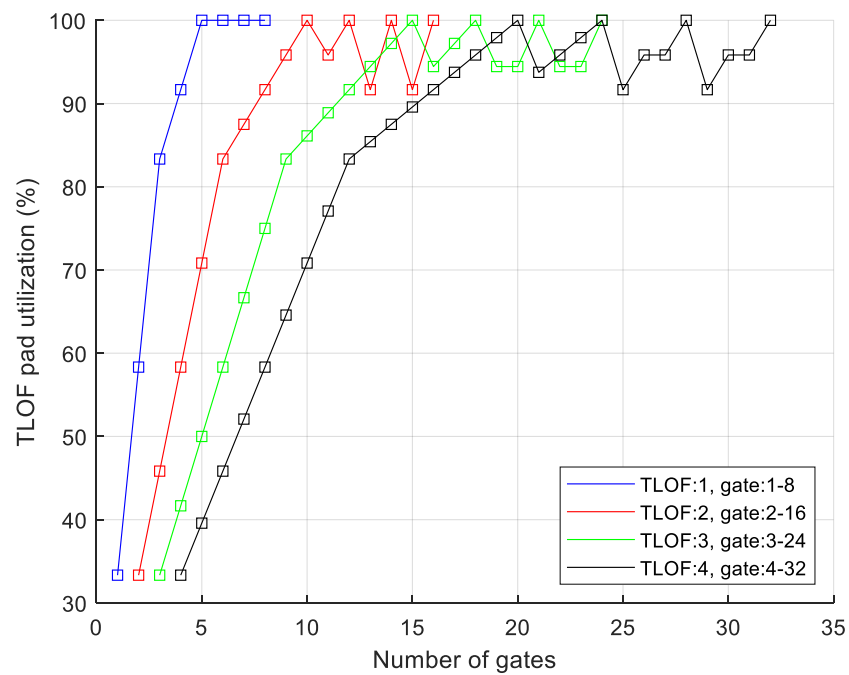


Figure 44. TLOF pad utilization according to TLOF pad and gate ratio.

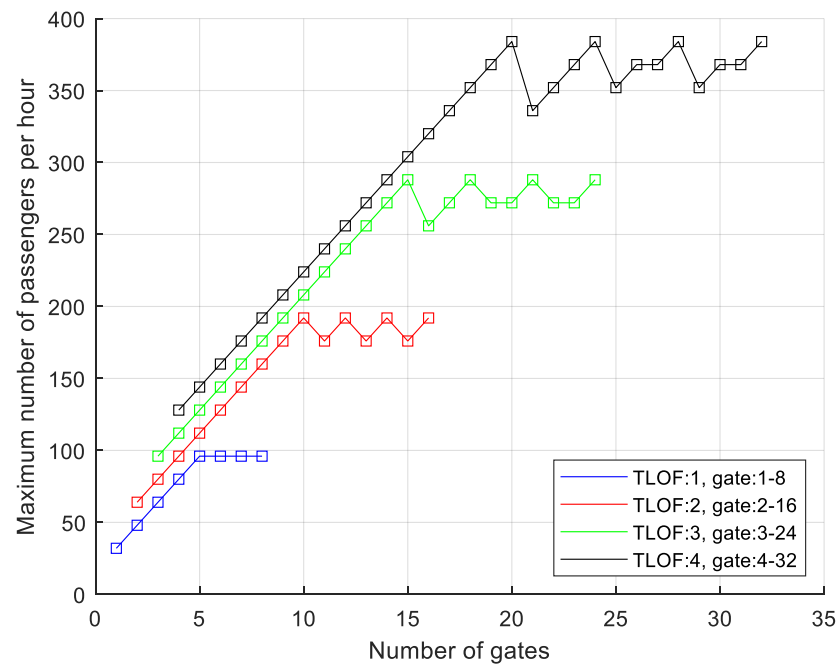


Figure 45. Maximum number of passengers per hour according to the TLOF pad and gate ratio.

5. Conclusions

In this paper, we studied the required site space and design criteria for a vertiport to efficiently utilize the limited available urban space in a UAM operation. Using the new FAA and EASA vertiport regulations issued in 2022, we studied the components and constraints of the vertiport, as well as the general characteristics of the linear, satellite, and pier topologies for the same area. Based on the K-UAM demonstration route, three types of vertiport layouts were applied to the parking lot of Gimpo Airport, which will be used as an airport shuttle vertiport in Seoul, and an efficient layout was proposed by analyzing the hourly capacity.

The size of the vertiport components depends on the size of the eVTOL aircraft to be operated, so the standard size of the vertiport components might vary. The vertiport component size was determined based on the relatively large Hyundai S-A1 eVTOL aircraft to be operated in Korea, which is the background of this study.

In this study, since a vertiport is to be installed and operated in a downtown area, the TLOF pad that requires a long taxiway was not considered. Results from this research can be used to validate the installation of a vertiport using hourly passenger demand calculated from the commuting population in the area.

By reviewing the utilization of the TLOF pad and gate, we can determine whether the installed vertiport has sufficient space to contain the components for efficient vertiport operation. Furthermore, if a different taxiing time is applied to each layout, a more realistic and accurate capacity can be obtained. In addition, if detailed characteristics such as the recharge time of the aircraft is considered with various eVTOL aircraft, the vertiport capacity can be calculated more accurately.

Author Contributions: Conceptualization, B.A.; methodology, B.A.; software, B.A.; validation, H.-Y.H.; formal analysis, B.A.; investigation, B.A.; resources, H.-Y.H.; data curation, B.A.; writing—original draft preparation, B.A.; writing—review and editing, H.-Y.H.; visualization, B.A.; supervision, H.-Y.H.; project administration, H.-Y.H.; funding acquisition, H.-Y.H. All authors have read and agreed to the published version of the manuscript.

Funding: This work is supported by a Korea Agency for Infrastructure Technology Advancement (KAIA) grant funded by the Ministry of Land, Infrastructure, and Transport (Grant 21CTAP-C157731-02).

Institutional Review Board Statement: Not applicable.

Informed Consent Statement: Not applicable.

Data Availability Statement: All data are available in the public.

Conflicts of Interest: The authors declare no conflict of interest.

References

1. Antcliff, K.R.; Moore, M.D.; Goodrich, K.H. Silicon Valley as an Early Adopter for On-Demand Civil VTOL Operations. In Proceedings of the 16th AIAA Aviation Technology, Integration, and Operations Conference, Washington, DC, USA, 13–17 June 2016.
2. Uber Connect. Available online: <https://www.corgan.com/story/uber-connect-evolved/> (accessed on 7 February 2022).
3. Pickard Chilton. Available online: <https://www.pickardchilton.com/work/uber-sky-tower> (accessed on 7 February 2022).
4. Gannett Fleming. Available online: <https://archello.com/project/skyport> (accessed on 7 February 2022).
5. Humphreys & Partners Architects. Available online: <https://humphreys.com/project/uber-elevate-2018/> (accessed on 7 February 2022).
6. BOKA Powell. Available online: <https://www.bokapowell.com/project/uber-air-2023-skyport-mobility-hub-concepts/> (accessed on 7 February 2022).
7. Vascik, P.D.; Hansman, R.J. Development of Vertiport Capacity Envelopes and Analysis of their Sensitivity to Topological and Operational Factors. In Proceedings of the 16th AIAA Aviation Technology, Integration, and Operations Conference, San Diego, CA, USA, 7–11 January 2019.
8. MATLAB. Available online: <https://kr.mathworks.com/products/matlab.html> (accessed on 7 February 2022).
9. Zelinski, S. Operational Analysis of Vertiport Surface Topology. In Proceedings of the 2020 AIAA/IEEE 39th Digital Avionics Systems Conference (DASC), San Antonio, TX, USA, 11–15 October 2020.
10. Federal Aviation Administration, Heliport Design, AC No: 150/5390-2C, 4/24/2012. Available online: https://www.faa.gov/airports/resources/advisory_circulars/index.cfm/go/document.current/documentnumber/150_5390-2 (accessed on 7 February 2022).
11. Gurreiro, N.M.; Butler, R.W.; Maddalon, J.M.; Hagen, G.E. Capacity and Throughput of Urban Air Mobility Vertiports with a First-Come, First-Served Vertiport Scheduling Algorithm. In Proceedings of the AIAA Aviation Forum, Virtual Event, 15–19 June 2020.
12. Vázquez, M.H. Vertiport Sizing and Layout Planning through Integer Programming in the Context of Urban Air Mobility. Master's Thesis, Technical University of Munich, Munich, Germany, 2021.
13. Schweiger, K.; Knabe, F.; Korn, B. An exemplary definition of a vertidrome's airside concept of operations. *Aerisp. Sci. Technol.* **2021**, *125*, 107144. [CrossRef]
14. Michael, A.P.; Meyers, P.E. Engineering Brief No. 105, Vertiport Design. Memorandum, Airport Engineering Division, AAS-100, Federal Aviation Administration, 2022. Available online: https://www.faa.gov/airports/engineering/engineering_briefs/drafts/media/eb-105-vertiport-design-industry-draft.pdf (accessed on 5 March 2022).

15. European Union Safety Agency. Prototype Technical Specifications for the Design of VFR Vertiports for Operation with Manned VTOL-Capable Aircraft Certified in the Enhanced Category. Vertiports, PTS-VPT-DSN, Cologne Germany, March 2022. Available online: <https://www.easa.europa.eu/document-library/general-publications/prototype-technical-design-specifications-vertiports> (accessed on 5 March 2022).
16. Smith, R.D. *Heliport/Vertiport Design Deliberations 1997–2000*; Federal Aviation Administration: Washington, DC, USA, 2001.
17. Federal Aviation Administration. Standard Specifications for Construction of Airports, AC No: 150/5370-10H, 12/21/2018. Available online: https://www.faa.gov/airports/resources/advisory_circulars/index.cfm/go/document.current/documentnumber/150_5370-10 (accessed on 7 February 2022).
18. Federal Aviation Administration. Air Traffic Control, ORDER JO 7110.65Z, 17 June 2021. Available online: https://www.faa.gov/regulations_policies/orders_notices/index.cfm/go/document.current/documentnumber/7110.65 (accessed on 7 February 2022).
19. SHoP Architecs. Available online: <https://www.shoparc.com/projects/uber-air/> (accessed on 7 February 2022).
20. Naver Map. Available online: <https://map.naver.com/v5/?c=14115800.6594852,4517340.1382280,16,0,0,0,dh> (accessed on 7 February 2022).
21. Korea Airports Corporation. Available online: https://www.youtube.com/watch?v=oFlb176OM5k&t=90s&ab_channel=%ED%95%9C%EA%B5%AD%EA%B3%B5%ED%95%AD%EA%B3%B5%EC%82%AC (accessed on 7 February 2022).
22. Parker, D. Vascik, Systems Analysis of Urban Air Mobility Operational Scaling. Ph.D. Thesis, Massachusetts Institute of Technology, Cambridge, MA, USA, 2020.